الجامعــة الأردنيــة
كلية الدراسات العليا

التاريخ: /   /

نموذج رقم (27)
تسليم رسالة ماجستير جامعية للمكتبة

الدكتور مدير المكتبـة

تحية طيبة وبعد،،،

لقد ناقش الطالب / الطالبة: يوسف محمد جبر علي البدوي   ورقمه الجامعي: 8070851

تخصص الماجستير: في الهندسة الميكانيكية

يوم: الخميس الموافق: 17 / 10 / 2010   ، وكانت النتيجة ناجحاً.

عنوان الرسالة (باللغة التي كتبت بها الرسالة)

MHD natural convection in iso-flux enclosures filled with porous medium

نرجو استلام النسخة الورقية التي تمت الموافقة عليها في صيغتها النهائية من قبل المشرف ولجنة المناقشة، ونسخة من الرسالة على القرص المضغوط (CD)، وذلك لإيداعها في المكتبة حسب الأصول.

وتفضلوا بقبول فائق الاحترام،،،

نائب عميد كلية الدراسات العليا	رئيس قسم التخصص أو نائب رئيس لجنة الدراسات العليا في كلية التخصص	المشرف
التوقيع:	التوقيع:	التوقيع: ....
التاريخ: / /	التاريخ: ١٠/١٠/ ٢٠١٠	التاريخ:٢٠١٠/١٠/١٩

مواصفات الاقراص المدمجة الخاصة بالرسائل الجامعية

- ان يضم القرص المدمج كافة المعلومات الواردة في النسخة الورقيه من الرسالة وذلك ضمن ملف واحد.
- ان يكون ترتيب الرسالة على القرص حسب ترتيب النسخة المطبوعة ورقيا.
- ان يحتوي القرص على صورة (save as jpg) عن اجازة الرسالة موقعة وموثقة من اعضاء لجنة المناقشة ومعتمدة من قبل الجامعة.
- تخزين الرسالة في ملف آخر على شكل (Acrobat reader PDF) لتسهيل تفعيل الرسالة على شبكة الانترنت ضمن قاعدة الرسائل الجامعية كاملة النص.

علما" أنه لن يكون بالامكان توثيق أي رسالة غير مطابقة للمواصفات المذكورة أعلاه.

الجامعة الأردنية
كلية الدراسات العليا

نموذج رقم (١٨)
اقرار والتزام بقوانين الجامعة الأردنية وأنظمتها
وتعليماتها لطلبة الماجستير والدكتوراة

أنا الطالب: يوسف محمد جبريل البريعي   الرقم الجامعي: 8070851

التخصص: الهندسة الميكانيكية   الكلية: الهندسة والتكنولوجيا

عنوان الرسالة / الاطروحة

MHD Natural Convection in iso – flux Enclosures filled with Porous media

أعلن بأنني قد التزمت بقوانين الجامعة الأردنية وأنظمتها وتعليماتها وقراراتها السارية المفعول المتعلقة باعداد رسائل الماجستير والدكتوراة عندما قمت شخصيا" باعداد رسالتي / اطروحتي ، وذلك بما ينسجم مع الأمانة العلمية المتعارف عليها في كتابة الرسائل والأطاريح العلمية. كما أنني أعلن بأن رسالتي /اطروحتي هذه غير منقولة أو مستلة من رسائل أو أطاريح أو كتب أو أبحاث أو أي منشورات علمية تم نشرها أو تخزينها في أي وسيلة اعلامية، وتأسيسا" على ما تقدم فإنني أتحمل المسؤولية بأنواعها كافة فيما لو تبين غير ذلك بما فيه حق مجلس العمداء في الجامعة الأردنية بالغاء قرار منحي الدرجة العلمية التي حصلت عليها وسحب شهادة التخرج مني بعد صدورها دون أن يكون لي أي حق في التظلم أو الاعتراض أو الطعن بأي صورة كانت في القرار الصادر عن مجلس العمداء بهذا الصدد.

توقيع الطالب: ....   التاريخ: ٢٠١٥ / ١٥ / ٢١

تعتمد كلية الدراسات العليا
هذه النسخة من الرسالة
التوقيع: .... التاريخ: ٢٠١٥/١/٢١

The University of Jordan

Authorization Form

I, Yousef Mohammed Jabir Al Badawi, authorize the University of Jordan to supply copies of my Thesis to libraries or establishments or individuals on request, according to the University of Jordan regulations.

Signature:

Date: October 17, 2010

MHD-NATURAL CONVECTION IN ISO-FLUX ENCLOSURES FILLED WITH POROUS MEDIA

By
Yousef Mohammed Al Badawi

Supervisor
Dr. Hamzeh M. Duwairi, Prof

This Thesis was Submitted in Partial Fulfillment of the Requirements for the Master's Degree of Science in Mechanical Engineering

**Faculty of Graduate Studies
The University of Jordan**

October, 2010

COMMETEE DECISION

This Thesis/Dissertation (MHD-NATURAL CONVECTION IN ISO-FLUX ENCLOSURES FILLED WITH POROUS MEDIA) was successfully defended and approved on October 17-2010.

Examination Committee   **Signature**
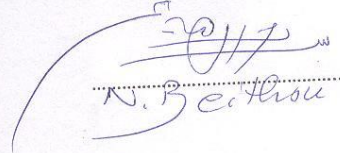
Dr. Hamzeh Duwairi (Supervisor)
Professor of thermal
(Jordan University)

Dr. Mahmoud Ahmad Hammad (Member)
Professor of thermal
(Jordan University)

Dr. Adnan W. Jaradat(Member)
Association Prof of thermal
(Jordan University)

Dr. N.Beithou (Member)
Association Prof of thermal
(Applied Science University)

DEDICATION

- **To my father, who has given his unlimited and unconditional love and care, without his support, I could not succeed.**

- **To my loving mother, whose presence has been my motivation.**

- **To my wife and my kids.**

- **To my brothers and sister.**

- **To all whom I love.**

ACNOWLEDGMENT

I want to thanks my Prof Hamzeh M.Duwairi in deep for his cooperation all over my work. I also would like to thanks extended to the committee: Prof. Mahmoud Ahmad Hammad, Dr. Adnan Jaradat and Dr. N.Beithou. . Finally, I want to thanks all those people who provided me with information, help, advice and support. And for all, we dedicate this project.

LIST OF CONTENTS:

Nomenclature

A   The aspect ratio of the enclosure.

$\vec{B}$ The magnetic field strength vector, [wb/ m^2]

B_0 magnatic field strength, [wb/ m^2]

C_F Forchheimer constant.

c_p Specific heat at constant pressure, [kJ/kg.K]

d   Diameter of spherical beads.[m]

$\vec{E}$ The electric field vector, [volt/ m]

$\vec{F}_e$ The magnetic force, [N]

$\vec{F}_{em}$ The total electromagnetic force, [N]

$\vec{F}_m$ The total electromagnetic force, [N]

Fr   Forchheimer number.

g   Gravitational acceleration, [m/ s^2]

Ge   The Gebhart number.

H   The length in y-direction, [m]

$\vec{H}$ The magnetic field intensity. [ampere/ m]

Ha^2 The magnetic influence number.

$\vec{J}$ The current density, [ampere/ area]

$\vec{J}_c$ The conduction current flow.

$\vec{J}_{md}$ The magnetic field induces a current in the conductor.

K   Permeability, [m^2]

k   Thermal conductivity of the porous media and fluid, [W/m.K]

P   Pressure, [Pa]

Ra_w Modified Rayleigh number.

T the fluid temperature, [K]

T_s Average surface temperature, [K]

u The velocity in x direction, [m/ s]

$\vec{V}$ The velocity of the conductor, [m/ s]

v The velocity in y direction, [m/ s]

W_{em} The work done on the system per unit time by the electromagnetic force, [Watt]

W The length in x-direction, [m]

Greek symbols

α_a Thermal diffusivity, $[m^2/ s]$

μ Absolute viscosity, [kg/m.s]

μ_0 The magnetic permeability.

ν Dynamic viscosity, $[m^2/ s]$

ε Porosity.

ρ The fluid density, $[kg/ m^3]$

ρ_0 The fluid density at some reference temperature, $[kg/ m^3]$

ρ_e The charge density.

σ Electrical conductivity, $[m\Omega/m^2]$

β Coefficient of thermal expansion, $[K^{-1}]$

$\emptyset$ The inclination angle of the enclosure, [degrees]

ψ Streamline function.

Ψ Dimensionless stream function.

Subscripts

i To describe the nodal points in the x-direction.

j To describe the nodal points in the y-direction.

N Number of nodal points in the y-direction.

M Number of nodal points in the x-direction.

Δx The increment in the x-direction.

Δy The increment in the y-direction.

centre The centre of the enclosure.

Mean The average Nusselt number.

MHD-NATURAL CONVECTION IN ISO-FLUX NCLOSURES FILLED WITH POROUS MEDIA

By
Yousef Mohammed Al Badawi

Supervisor
Dr. Hamzeh M. Duwairi, Prof

ABSTRACT

In this present study the magnetohydrodynamics (MHD) natural convection iso-flux problem inside a porous media filled inclined rectangular enclosures is studied numerically. An iso-heat flux is applied for heating the two opposing walls of the enclosure while the other two walls are adiabatic. The Forchheimer extension of Darcy-Oberbeck-Boussinesq and energy equations are going to be transformed into dimensionless form using a set of suitable variables then solved by using a finite difference scheme. Governing parameters are the magnetic influence number, the Rayleigh number, the inclination angle, and the aspect ratio of the enclosure. It is found that when the increasing of (Ha^2)decreases the heat transfer coefficient and the fluid flow velocities, which is due to unfavorable retarding forces between the fluid layers, the increasing the (Ge) number decreases heat transfer rates, the Maximum heat transfer rates are obtained for inclination angels nearly 60°,and the increasing the (For) number decreases the Nusselt number .

Chapter 1
Introduction

1.1   Introduction:

The Darcy effects on natural convection in porous media have received a great deal of attention in recent years. This is due to a large number of technical applications, such as, fluid flow in geothermal reservoirs, separation processes in chemical industries, dispersion of chemical contaminants through water saturated soil, solidification of casting, migration of moisture in grain storage system, crude oil production, etc.[Nield].

The study of fluid, which is electrically conducted and moves in a magnetic field, is known as a magneto hydrodynamics (MHD), the generated current interacts with the magnetic field to produce a body force on the fluid.

1.2 **Momentum equation and Porous medium**

Flow in porous medium is generalized by Darcy's law. It shows the volumetric flow rate is a function of the flow area, elevation and fluid pressure. It may be stated in several different forms depending on the flow conditions. Since its discovery, it has been found valid for any Newtonian fluid, while it was established under saturated flow conditions, it may be adjusted to account for unsaturated and multiphase flow this is expressed, in refined form, by:-

$$u = -\frac{K}{\mu}\frac{\partial P}{\partial x} \qquad (1.1)$$

where K is Permeability, which is a measure of the ease with which fluids may transfer through medium under the influence of a driving pressure, $\frac{\partial P}{\partial x}$ is the pressure gradient in the flow direction and μ is the dynamic viscosity of the fluid.

Darcy's equation (1.1) is linear in the velocity u, it holds when u is sufficiently small. In practice, "sufficiently small" means that is of order unity or smaller. As u increases, the transition to nonlinear drag is quite smooth; there is no sudden transition as Re is increased in the range 1 to 10. Clearly this transition is not one from laminar to turbulent flow, since at such comparatively small Reynolds numbers the flow in the pores is still laminar. Rather, the breakdown in linearity is due to the fact that the form drag due to solid obstacles is now comparable with the surface drag due to friction. The appropriate modification to Darcy's equation is to replace Eq. (1.1) by

$$u = -\frac{K}{\mu}\frac{\partial P}{\partial x} + \frac{C_F \rho}{\sqrt{K}}u^2 \tag{1.2}$$

where C_F is Forcheimer constant and where ρ is the fluid density and K is permeability of the porous medium.

1.3 MHD Flow

The research of MHD in porous medium has been conducted widely in recent years, which involves post-accidental heat rem

oval in nuclear reactors, cooling of radioactive waste containers, the migration of moisture through the air contained in fibrous insulations, heat exchangers, solar power collectors, grain storage, energy efficient drying process, electrical discharges, and many others. Some basic electromagnetic concept as follows:

For a neutrally charged system the current density $\vec{J}$ is given by:

$$\vec{J} = \sigma.\vec{E} \tag{1.3}$$

where σ is the electrical conductivity and $\vec{E}$ is the electric field vector. The magnetic field strength $\vec{B}$ is expressed by:

$$\vec{B} = \mu_0.\vec{H} \tag{1.4}$$

where μ_0 is called the magnetic permeability and $\vec{H}$ is the Magnetic field intensity. The force exerted on a system of charged particles by an electric field is given by:

$$\vec{F}_e = \rho_e.\vec{E} \tag{1.5}$$

where ρ_e is the charge density. The magnetic force exerted on a current is expressed by:

$$\vec{F}_m = \vec{J} \times \vec{B} \tag{1.6}$$

The total electromagnetic force is given by:

$$\vec{F}_{em} = \rho_e.\vec{E} + \vec{J} \times \vec{B} \tag{1.7}$$

The power done on the system per unit time by the electromagnetic force is expressed by:

$$W_{em} = \vec{F}_{em}.\vec{V} \tag{1.8}$$

where V is the velocity of the conductor.

The magnetic field induces a current in the conductor is given by:

$$\vec{J}_{md} = \sigma(\vec{V} \times \vec{B}) \tag{1.9}$$

Then, the conduction current flow is given by:

$$\vec{J}_c = \sigma(\vec{E} + \vec{V} \times \vec{B}) \tag{1.10}$$

And the total current flow is given by:

$$\vec{J} = \vec{J}_c + \rho_e.\vec{V} \tag{1.11}$$

For the electromagnetic work Holman (1990):

$$W_{em} = \vec{E}.\vec{J} - \frac{\vec{J}_c.\vec{J}_c}{\sigma} \tag{1.12}$$

The governing equations that describe the problem under consideration can be written

as: The continuity equation: [Bilgen et al]

$$\frac{\partial u}{\partial x} + \frac{\partial v}{\partial y} = 0 \tag{1.13}$$

The momentum equation in x and y-directions: [Bilgen et al]

$$\frac{\mu u}{K} + \frac{\rho C_F}{\sqrt{K}} u^2 + \sigma B_0^2 u = -\frac{\partial P}{\partial x} + \rho \beta g (T_s - T) \cos \phi \qquad (1.14)$$

$$\frac{\mu v}{K} + \frac{\rho C_F}{\sqrt{K}} v^2 + \sigma B_0^2 v = -\frac{\partial P}{\partial y} + \rho \beta g (T_s - T) \sin \phi \qquad (1.15)$$

The energy equation: [Bilgen et al]

$$u\frac{\partial T}{\partial x} + v\frac{\partial T}{\partial y} = \frac{k}{\rho c_p}\left(\frac{\partial^2 (T_s - T)}{\partial x^2} + \frac{\partial^2 (T_s - T)}{\partial y^2}\right) + \frac{\nu}{K c_p} u \left(u + \frac{C_F \sqrt{K}}{\nu} u^2\right) + \frac{\sigma B_0^2}{\rho c_p} u^2 \quad (1.16)$$

where:-

- T: The fluid temperature.

- T_S: Average surface temperature.

- The term (σB_0^2) represents the effect of magnetic field force.

- The term $(\frac{\sigma B_0^2}{\rho c_p})$ represents the work done by magnetic field force.

- ϕ : is inclination angle of the enclosure.

1.4 Boussinesq Approximation:

In this case we add the gravitational term ρg to the right-hand side of the Forchheimer's equation (1.2) to show the convection heat transfer effect, the density of the fluid must be a function of the temperature, and hence we need an equation of state to complement the equations of mass, momentum, and energy. When temperature is changed the density of a fluid can be expressed as:

$$\rho = \rho_0\big(1 + \beta(T - T_0)\big) \tag{1.17}$$

where ρ_0 is the fluid density at some reference temperature T_0 and β is the coefficient of thermal expansion. Joseph Boussinesq (1903) was the first practitioner of buoyancy-driven flows for small density and temperature differences in the fluid. The approximation consists of setting constants all the properties of the medium, except that the vital buoyancy term involving β is retained in the momentum equation.

Chapter 2

Literature Review

2.1 **Introductions**

Geothermal operation, nuclear reactors, transportation, separation processes in chemical industries, cooling building thermal insulation, are well-known applications of the extensive studies on the porous media flow and heat transfer, which has been started by Darcy, in the 19th century.

2.1.1 Internal flow

Kim and Lee (2000) set up an experiment using a circular cylinder where electrodes and magnets are installed in an alternative sequence in axial direction of the cylinder to generate magnetic force in the circumferential direction. It is found that the thermal boundary layer is developed near the bottom and side walls and the central regime near the top surface has least temperature gradient for both uniform and non-uniform heating cases.

Garandet et al. (1992) had analyzed the equations of the magneto hydrodynamics that can be used to model the effect of a transverse magnetic field on the buoyancy driven convection in a two dimensional cavity. It is found that with the increase of magnetic field intensity, the magnetic force has more effects on the nonmetallic materials.

Kumar and Kumar have conducted (2002) a numerical study on natural convection in porous trapezoidal enclosures using finite element method, they indicated that Nusselt number increases with the increasing angle of inclination of the walls of the trapezoidal enclosures.

Baytas and Pop (1999) performed a numerical analysis to investigate the natural convection in a porous trapezoidal enclosure. They solved the Darcy and energy equations using alternative Direction Implicit finite-difference method. They indicated that conduction heat transfer regime is dominated for low Rayleigh numbers. The same method was used to investigate free convection in oblique enclosures filled

with a porous medium in their other study. They observed that near the sharp corners of the oblique enclosure the flow and temperature break down into a series of sub vortices.

Duwairi and Shehadah (2008) have studied the MHD natural convection heat transfer problem inside a porous medium. Two sides of the rectangular enclosure are adiabatic and the other two are isothermal. Three-parameters are found to describe the problem under consideration, namely: the buoyancy parameter, the inclination angle parameter, and the magnetic effect parameter of the rectangular porous media-filled enclosure.

2.1.2 External flow

Badruddin et al. (2006) have studied the steady state heat transfer in a porous medium fixed in a vertical annular cylinder. The Darcy model of flow was employed and heat transfer was assumed to take place by natural convection and radiation. The governing equations were solved using the finite element method. They found that if interphase heat transfer coefficient and modified conductivity ratio are maintained at high values, then thermal equilibrium is approached with both solid and fluid phases having similar temperatures.

 Sparrow and Cess (1961) have investigated the free convection heat transfer due to the simultaneous action of buoyancy and induced magnetic forces; the analysis is carried out for laminar boundary-layer flow about an isothermal vertical plate. They found that the free convection heat transfer to liquid metals may be significantly affected by the presence of magnetic field, but that very small effects are experienced by other fluid.

.Raptis and Singh (1983) studied the effect of a uniform transform transverse magnetic field on the free convection flow of an electrically conducting fluid past an infinite vertical plate for classes of impulsive as well as uniformly accelerated motion of the plate. They found that the effect of the magnetic field

is to increase the velocity field on both cases. Henoch and Meng (1991) used the magnetic force to retard the transition to the turbulent boundary layer and reduce the frictional Darcy force.

Hossain. Aldoss et al (1992) had studied the effect of viscous and Joule heating on the flow of an electrically conducting and viscous incompressible fluid past a semi-infinite plate of which temperature varies linearly with the distance from the leading edge and in the presence of uniform transverse magnetic field. The equations governing the flow are solved numerically applying the finite difference method along with Newton's linearization approximation. The combined effects of forced and natural convection heat transfer in the presence of transverse magnetic field from vertical surfaces are studied by many researchers.

Jha (2001) has discussed the combined effect of natural convection and uniform transverse magnetic field on the Couette flow of an electrically conducting fluid between two parallel plates for impulsive motion of one plate. Comparative study is made between rile velocity field for magnetic field fixed with respect to plate and a fixed magnetic field with respect to the fluid.

On other study, the effects of MHD-natural convection heat transfer from radiating vertical porous surfaces, they found non-similarity parameter to solve this problem with fluid suction or injection along the stream wise coordinate and found that the increasing of the magnetic field strength decreases the velocity and the heat transfer rates inside the boundary laye had studied by Duwairi and Damseh (2004, a).

Duwairi and Duwairi (2004, b) studied the thermal radiation heat transfer effects on the MHD-Rayleigh flow of gray viscous fluids under the effect of a transverse magnetic field, the free convection heat transfer problem from constant surface heat flux moving plate is selected for study. They found that the increasing of the magnetic field strength decreased the velocity inside the boundary layer. Duwairi and Al-Araj (2004, c) studied the MHD-thermal radiation interaction along a vertical cylinder embedded in a

plain medium; they found that the increasing of magnetic forces decreased velocities and heat transfer rates to the conductive fluids. The MHD-conjugative heat transfer problem from vertical surfaces embedded in saturated porous media; the inclusion of conduction parameter to the MHD traditional mixed convection problem is achieved has been formulated by Duwairi and Al-Kablawi (2006).

Duwairi et al. (2006) studied the transient MHD natural convection heat transfer problem using non-Boussinesq approximation. Hammad and Duwairi (2008) had been solved the non-Newtonian MHD convection heat transfer problem around a non isothermal cylinder and spheres. Again the magnetic forces had retarding effects on the flow and heating effect of the fluid layers, which had decreased the local Nusselt numbers,

In all the previous studied the MHD effects for externally flow are investigated either for fluid flow in a plain or a porous media, but little attention is given to the internal flow heat flux problem in. In the present study, the magnetohydrodynamics(MHD) natural convection heat transfer effect inside an iso-flux porous medium- filled inclined rectangular enclosures has been investigated numerically. An iso-heat flux is applied for heating the two opposing walls of the enclosure while the other walls are adiabatic. The governing equations, continuity, Forchheimer extension of Darcy law and energy, are going to be transformed into dimensionless form using a set of suitable variables and then solved using a finite difference scheme. Governing parameters are magnetic effect, Gebhart number, Darcy Rayleigh number, inclination angle, and the aspect ratio of the enclosure.

Chapter 3

Problem Formulations

3.1 Introduction:

In recent years a large number of analytical studies have been performed relating to the problem of MHD natural convection with filled enclosure and porous media. In this study the magneto hydrodynamics natural convection heat flux problem inside a porous media filled inclined rectangular enclosures is going to be studied. One wall of the enclosure is kept at a constant heat flux q_1 and the opposite is kept at heat flux q_2. The other two walls of the enclosure are adiabatic, i.e., it is assumed that no heat is transferred into or out of walls.

3.2 Governing equations:

In present work, consider the inclined rectangular enclosure, which is embedded in a fluid-saturated porous media as shown in figure (3.1). In order to obtain the governing equation, some assumptions were made as following:-

- The flow is steady and two dimensional.
- The thermo physical properties of the fluid are homogeneous and isotropic.
- The temperature of the fluid is everywhere below the boiling point.
- The magnetic field is uniform throughout the boundary layer.
- The fluid inside the enclosure is incompressible fluid.

Under these assumptions the governing equations which describe the problem are:

The continuity equation:

$$\frac{\partial u}{\partial x} + \frac{\partial v}{\partial y} = 0 \tag{3.1}$$

The momentum equation in x and y-directions:

$$\frac{\mu u}{K} + \frac{\rho C_F}{\sqrt{K}} u^2 + \frac{\sigma B_{0x}^2}{K} u = -\frac{\partial P}{\partial x} + \rho \beta g (T_s - T) \cos \phi \tag{3.2}$$

$$\frac{\mu v}{K} + \frac{\rho C_F}{\sqrt{K}} v^2 + \frac{\sigma B_{0y}^2}{K} v = -\frac{\partial P}{\partial y} + \rho \beta g (T_s - T) \sin \phi \tag{3.3}$$

The energy equation:

$$u \frac{\partial T}{\partial x} + v \frac{\partial T}{\partial y} = \frac{k}{\rho c_p} \left(\frac{\partial^2 T}{\partial x^2} + \frac{\partial^2 T}{\partial y^2} \right) + \frac{\nu}{K c_p} u \left(u + \frac{C_F \sqrt{K}}{\nu} u^2 \right) + \frac{\sigma B_0^2}{\rho c_p} u^2 \tag{3.4}$$

where x and y are the distances measured along the horizontal and vertical directions, respectively ϕ is inclination angle of the enclosure, respectively; u and v are the velocity components in the x- and y- directions, respectively, the gravitational acceleration g is acting downward in the Earth. Six-parameters are found to describe the problem under consideration namely;

a. $(\frac{\mu u}{K})$: The Darcy effect parameter.

b. g:The gravitational effect parameter.

c. ϕ:inclination angle parameter.

d. $(\frac{\sigma B_{0x}^2}{K} u)$ and $(\frac{\sigma B_{0y}^2}{K} v)$: magnetic effect parameter.

e. $(\frac{\nu}{K c_p} u \left(u + \frac{C_F \sqrt{K}}{\nu} u^2 \right))$ The viscous heating effect parameter.

f. $(\frac{\sigma B_{0x}^2}{\rho K c_p} u^2)$: The Joule heating effect parameter.

The boundary conditions for the flow in the enclosure are:

.

In the left hand side wall $\qquad x = 0, \ u = 0, - k \frac{\partial T}{\partial x}\Big|_{x=0} = q_1$

In the right hand side wall $\qquad x = W, \ u = 0, - k \frac{\partial T}{\partial x}\Big|_{x=W} = q_2$

In the upper adiabatic wall $\qquad y = H, \ v = 0, - k \frac{\partial T}{\partial y}\Big|_{y=H} = 0$

In the lower adiabatic wall $\qquad y = 0, \ v = 0, - k \frac{\partial T}{\partial y}\Big|_{y=0} = 0$

$$(3.5)$$

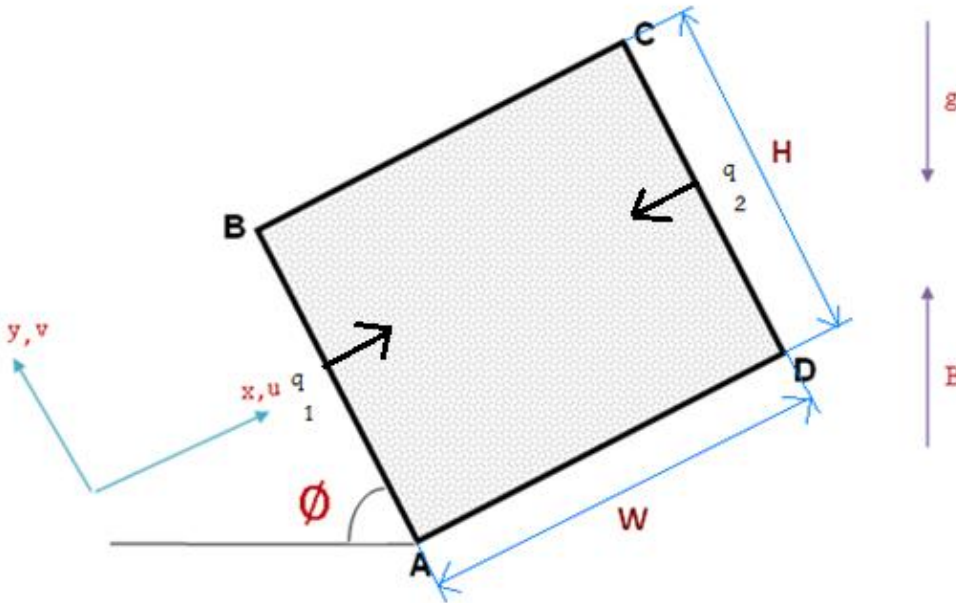where W and H is the width and the length of the enclosure as shown in figure (3.1).

Figure 3.1 Schematic of physical model and coordinate system

3.3 dimensionless forms of governing equations

The numerical solutions are obtained in terms of the velocity components (u,v) and stream function ψ is evaluated using the relationship between the stream function ψ and the velocity components [Batchelor], where the stream function ψ is defined as:

$$u = \frac{\partial \psi}{\partial y}, v = -\frac{\partial \psi}{\partial x} \qquad (3.6)$$

It may be noted that, the positive sign of ψ denotes anti-clockwise circulation and the clockwise circulation is represented by the negative sign of ψ.In terms of the stream function, the continuity equation, i.e., Eq. (3.1) is:

$$\frac{\partial^2 \psi}{\partial x \, \partial y} - \frac{\partial^2 \psi}{\partial x \, \partial y} = 0 \tag{3.7}$$

Derivation the momentum equation in x and y-directions, i.e., Eq. (3.2) and (3.3), with respect to y and x respectively and by subtracting the resulting equations, the pressure is eliminated and the following equation is obtained:

$$\frac{\mu}{K}\left(\frac{\partial u}{\partial y} - \frac{\partial v}{\partial x}\right) + \frac{\rho C_F}{\sqrt{K}}\frac{\partial u^2}{\partial y} + \frac{\sigma B_0^2}{K}\left(\frac{\partial u}{\partial y}\sin\phi - \frac{\partial v}{\partial x}\cos\phi\right) =$$

$$\rho \beta g \left(\frac{\partial (T_s - T)}{\partial y}\cos\phi - \frac{\partial (T_s - T)}{\partial x}\sin\phi\right) \tag{3.8}$$

Using the definition of the stream function, Eq. (3.8) becomes:

$$\frac{\partial^2 \psi}{\partial x^2} + \frac{\partial^2 \psi}{\partial y^2} + \frac{2C_F \sqrt{K}}{\nu}\frac{\partial \psi}{\partial y}\frac{\partial^2 \psi}{\partial y^2} + \frac{K\sigma B_0^2}{\mu}\left(\frac{\partial^2 \psi}{\partial y^2}\sin\phi + \frac{\partial^2 \psi}{\partial x^2}\cos\phi\right) =$$

$$\frac{\rho \beta g K}{\mu}\left(\frac{\partial (T_s - T)}{\partial y}\cos\phi - \frac{\partial (T_s - T)}{\partial x}\sin\phi\right) \tag{3.9}$$

In terms of the stream function, the energy equation, i.e., Eq. (3.4) is:

$$\frac{\partial \psi}{\partial y}\frac{\partial (T_S - T)}{\partial x} - \frac{\partial \psi}{\partial x}\frac{\partial (T_S - T)}{\partial y} = \frac{k}{\rho c_p}\left(\frac{\partial^2 (T_S - T)}{\partial x^2} + \frac{\partial^2 (T_S - T)}{\partial y^2}\right) +$$

$$\frac{\nu}{Kc_p}\frac{\partial \psi}{\partial y}\left(\frac{\partial \psi}{\partial y} + \frac{C_F\sqrt{K}}{\nu}\left(\frac{\partial \psi}{\partial y}\right)^2\right) + \frac{\sigma B_0^2}{\rho c_p}\left(\frac{\partial \psi}{\partial y}\right)^2 \qquad (3.10)$$

The non-dimensional parameters are listed as

$$X = \frac{x}{W}, Y = \frac{y}{W}, \Psi = \frac{\psi}{\alpha_a}, \theta = \frac{T_S - T}{\frac{q_1 W}{k_a}} \qquad (3.11)$$

where, as before, the apparent thermal diffusivity of the porous material, α_a is equal to $\left(\frac{k_a}{\rho c_p}\right)$.

In terms of variables defined in Eq. (3.11), Eq. (3.10) and (3.9) become:

$$\frac{\partial^2 \Psi}{\partial X^2} + \frac{\partial^2 \Psi}{\partial Y^2} + 2For\frac{\partial \Psi}{\partial Y}\frac{\partial^2 \Psi}{\partial Y^2} + Ha^2\left(\frac{\partial^2 \Psi}{\partial Y^2}\sin\phi + \frac{\partial^2 \Psi}{\partial X^2}\cos\phi\right) =$$

$$Ra_w\left(\frac{\partial \theta}{\partial Y}\cos\phi - \frac{\partial \theta}{\partial X}\sin\phi\right) \qquad (3.12)$$

$$\frac{\partial \Psi}{\partial Y}\frac{\partial \theta}{\partial X} - \frac{\partial \Psi}{\partial X}\frac{\partial \theta}{\partial Y} = \frac{\partial^2 \theta}{\partial X^2} + \frac{\partial^2 \theta}{\partial Y^2} + Ge\frac{\partial \Psi}{\partial Y}\left(\frac{\partial \Psi}{\partial Y} + For\left(\frac{\partial \Psi}{\partial Y}\right)^2\right)$$

$$+(Ge)(Ha^2)\left(\frac{\partial \Psi}{\partial Y}\right)^2 \qquad (3.13)$$

where Ra_w is the modified Rayleigh number based on the enclosure width W, i.e.:

$$Ra_w = \frac{\beta g K q_1 W^2}{\alpha_a \nu k_a} \tag{3.14}$$

Fr is the Forchheimer number based on the enclosure width W, i.e.:

$$For = \frac{C_F \alpha_a \sqrt{K}}{\nu W} \tag{3.15}$$

Ha^2 is the magnetic influence number, i.e.:

$$Ha^2 = \frac{K \sigma B_0^2}{\mu} \tag{3.16}$$

and Ge is the Gebhart number, i.e.:

$$Ge = \frac{\nu \alpha_a k_a}{K c_p q_1 w} \tag{3.17}$$

the boundary conditions In terms of dimensionless variables defined in Eq. (3.11), are:

1. Iso-flux walls

$$\left. \frac{d\theta}{dX} \right|_{X=0} = -1 \quad , \qquad \left. \frac{d\theta}{dX} \right|_{X=1} = \frac{q_2}{q_1} \tag{3.18}$$

2. Adiabatic walls

$$\frac{\partial \theta}{\partial Y} = 0 \qquad at \; Y = 0 \; and \; Y = A \tag{3.19}$$

where A=H/W is the aspect ratio of the enclosure.

In terms of the stream function, the boundary conditions on the velocity component normal to wall are:

$$\frac{\partial \psi}{\partial x} = 0 \qquad \text{at } x = 0 \text{ and } x = W$$

$$\frac{\partial \psi}{\partial y} = 0 \qquad \text{at } y = 0 \text{ and } y = H \qquad (3.20)$$

The absolute value of the stream function will arbitrarily be assumed that the stream function has a value of 0 at the point A shown in fig. (3.1).the boundary conditions ψ is 0 at point A, it is zero everywhere along AB. and BC in the walls boundary In similar way, it can be deduced that ψ is 0 everywhere along CD and DA.

Chapter 4
Numerical Solution

4.1 Introduction:

In recent years a large number of numerical methods have been developed for the solving of boundary layer equations, such as the finite difference method, Galerkin method, and finite element method. Of these, the finite difference method is at present the most common for boundary layer equations. Many different finite difference representations are possible for any given partial differential equation; derivatives are approximated by finite difference resulting in an algebraic representation of the partial differential equation.

.
4.2 Discretization of governing equations

Finite difference method is used to solve governing equations by using central difference method is applied for discretization of equations, basically identical to that used before to solve for a flow in a fluid-filled enclosure, will be discussed. If a uniformly spaced grid is used and if attention is directed to the grid points, as shown in fig. (4.1), the following finite-difference form of Eq. (3.13) is obtained:

$$\left[\frac{\Psi_{i,j+1}-\Psi_{i,j-1}}{2\Delta Y}\right]\left[\frac{\theta_{i+1,j}-\theta_{i-1,j}}{2\Delta X}\right] - \left[\frac{\Psi_{i+1,j}-\Psi_{i-1,j}}{2\Delta X}\right]\left[\frac{\theta_{i,j+1}-\theta_{i,j-1}}{2\Delta Y}\right] = \left[\frac{\theta_{i+1,j}-2\theta_{i,j}+\theta_{i-1,j}}{\Delta X^2}\right] + \left[\frac{\theta_{i,j+1}-2\theta_{i,j}+\theta_{i,j-1}}{\Delta Y^2}\right] +$$

$$\text{Ge}\left[\frac{\Psi_{i,j+1}-\Psi_{i,j-1}}{2\Delta Y}\right]\left[\left[\frac{\Psi_{i,j+1}-\Psi_{i,j-1}}{2\Delta Y}\right] + \text{For}\left[\frac{\Psi_{i,j+1}-\Psi_{i,j-1}}{2\Delta Y}\right]^2\right] + (\text{Ge})(\text{Ha}^2)\left[\frac{\Psi_{i,j+1}-\Psi_{i,j-1}}{2\Delta Y}\right]^2$$
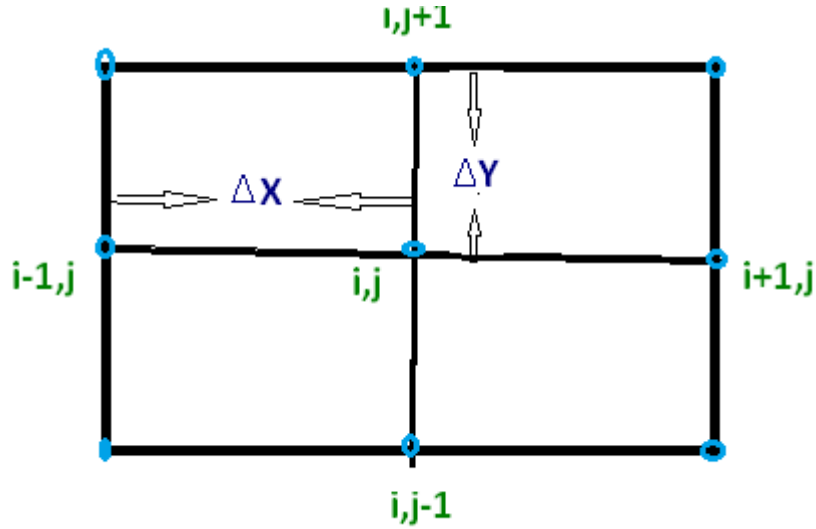
(4.1)

Fig. 4.1 Nodal points used.

The first guessed values are necessary used in iterative procedure to updated the values and

repeat the process until convergence is attained , The above equation is written in term of the

stream function defined as:-

$$\theta_{i,j} = \left\{\left(\frac{\theta_{i+1,j} + \theta_{i-1,j}}{\Delta X^2}\right) + \left(\frac{\theta_{i,j+1} + \theta_{i,j-1}}{\Delta Y^2}\right) + (Ge)(Ha^2)\left(\frac{\Psi_{i,j+1} - \Psi_{i,j-1}}{2\Delta Y}\right)^2\right.$$

$$+ Ge\left(\frac{\Psi_{i,j+1} - \Psi_{i,j-1}}{2\Delta Y}\right)\left[\left(\frac{\Psi_{i,j+1} - \Psi_{i,j-1}}{2\Delta Y}\right) + For\left(\frac{\Psi_{i,j+1} - \Psi_{i,j-1}}{2\Delta Y}\right)^2\right]$$

$$\left. + \left(\frac{\Psi_{i+1,j} - \Psi_{i-1,j}}{2\Delta X}\right)\left(\frac{\theta_{i,j+1} - \theta_{i,j-1}}{2\Delta Y}\right) - \left(\frac{\Psi_{i,j+1} - \Psi_{i,j-1}}{2\Delta Y}\right)\left(\frac{\theta_{i+1,j} - \theta_{i-1,j}}{2\Delta X}\right)\right\}/\left(\frac{2}{\Delta X^2} + \frac{2}{\Delta Y^2}\right) \tag{4.2}$$

The right-hand side of this equation is calculated using the "most recent" values of the variables.

Under-relaxation is actually used so the updated value of θ is given by:

$$\theta_{i,j}^1 = \theta_{i,j}^0 + r\left(\theta_{i,j}^{calc} - \theta_{i,j}^0\right) \tag{4.3}$$

Where $\theta_{i,j}^0$ is the value of $\theta_{i,j}$ at the previous iteration and $\theta_{i,j}^{calc}$ is the value given by Eq. (4.2) , r

(< 1) is again the under-relaxation parameter.

4.3 Second order accuracy of the boundary conditions

The boundary conditions determine the dimensionless temperatures on the walls.

For first order give:

$$j = 1,2, ..., N: \quad \theta_{1,j} = \theta_{2,j} + \Delta X, \quad \theta_{M,j} = \frac{q_2}{q_1} \Delta X + \theta_{M-1,j} \tag{4.4.a}$$

For Second order

$$j = 1,2, ..., N: \quad \theta_{1,j} = 4 * \theta_{2,j} - \theta_{3,j} + 2 * \frac{\Delta X}{3}, \quad \theta_{M,j} = \frac{q_2}{q_1} * 2 * \Delta X$$

$$+ 4 * \theta_{M-1,j} - \frac{\theta_{M-2,j}}{3} \tag{4.4.b}$$

There being N nodal points in Y-direction and M in X-direction. On the other two walls, since

the gradient in the Y-direction is zero.

to first order accuracy:

$$i = 1,2, ..., M: \quad \theta_{i,1} = \theta_{i,2}, \quad \theta_{i,N} = \theta_{i,N-1} \tag{4.5.a}$$

to second order accuracy:

$$i = 1,2, ..., M: \quad \theta_{i,1} = 4 * \theta_{i,2} - \frac{\theta_{i,3}}{3}, \quad \theta_{i,N} = 4 * \theta_{i,N-1} - \frac{\theta_{i,N-1}}{3} \tag{4.4.b}$$

The stream function equation, i.e., Eq. (3.12), is treated in the same way as the energy equation.

The following finite-difference form of Eq. (3.12) is, therefore, obtained:

$$\left[\frac{\Psi_{i,j+1}-2\Psi_{i,j}+\Psi_{i,j-1}}{\Delta Y^2}\right] + \left[\frac{\Psi_{i+1,j}-2\Psi_{i,j}+\Psi_{i-1,j}}{\Delta X^2}\right] + 2\text{For}\left[\frac{\Psi_{i,j+1}-\Psi_{i,j-1}}{2\Delta Y}\right]\left[\frac{\Psi_{i,j+1}-2\Psi_{i,j}+\Psi_{i,j-1}}{\Delta Y^2}\right] +$$

$$\text{Ha}^2\left[\frac{\Psi_{i,j+1}-2\Psi_{i,j}+\Psi_{i,j-1}}{\Delta Y^2}\sin\emptyset + \frac{\Psi_{i+1,j}-2\Psi_{i,j}+\Psi_{i-1,j}}{\Delta X^2}\cos\emptyset\right] = \text{Ra}_w\left[\frac{\theta_{i,j+1}-\theta_{i,j-1}}{2\Delta Y}\cos\emptyset - \frac{\theta_{i+1,j}-\theta_{i-1,j}}{2\Delta X}\sin\emptyset\right]$$

(4.6)

$$\Psi_{i,j} = \left\{\left(\frac{\Psi_{i,j+1}+\Psi_{i,j-1}}{\Delta Y^2}\right) + \left(\frac{\Psi_{i+1,j}+\Psi_{i-1,j}}{\Delta X^2}\right) + 2\text{For}\left(\frac{\Psi_{i,j+1}-\Psi_{i,j-1}}{2\Delta Y}\right)\left(\frac{\Psi_{i,j+1}+\Psi_{i,j-1}}{\Delta Y^2}\right)\right.$$

$$+\text{Ha}^2\left(\frac{\Psi_{i,j+1}+\Psi_{i,j-1}}{\Delta Y^2}\sin\emptyset + \frac{\Psi_{i+1,j}+\Psi_{i-1,j}}{\Delta X^2}\cos\emptyset\right) - \text{Ra}_w\left(\frac{\theta_{i,j+1}-\theta_{i,j-1}}{2\Delta Y}\cos\emptyset - \right.$$

$$\left.\left.\frac{\theta_{i+1,j}-\theta_{i-1,j}}{2\Delta X}\sin\emptyset\right)\right\}/\left\{\frac{2}{\Delta Y^2} + \frac{2}{\Delta X^2} + \frac{2\text{Fr}}{\Delta Y^2}\left(\frac{\Psi_{i,j+1}-\Psi_{i,j-1}}{\Delta Y}\right) + \frac{2\text{Ha}^2}{\Delta X^2}\sin\emptyset + \frac{2\text{Ha}^2}{\Delta Y^2}\cos\emptyset\right\}$$

(4.7)

The relaxation is also again used so the updated value of i, j is actually given by:

$$\Psi_{i,j}^1 = \Psi_{i,j}^0 + r\left(\Psi_{i,j}^{\text{calc}} - \Psi_{i,j}^0\right) \tag{4.8}$$

where $\Psi_{i,j}^{\text{calc}}$ is the value given by Eq. (4.7) and $\Psi_{i,j}^0$ is the value of $\Psi_{i,j}$ at the previous iteration. r (< 1) is again the under-relaxation parameter.

Eq. (4.7) is applied at all "internal" nodal points. The boundary conditions have the value of' $\Psi = 0$ on all boundary points, i.e.:

$$j = 1,2,\dots,\text{N}: \quad \Psi_{i,j} = 0, 1, \Psi_{M,j} = 0$$

$$i = 1,2,\dots,\text{M}: \quad \Psi_{i,j} = 0, 1, \Psi_{i,N} = 0 \tag{4.9}$$

The above procedure is actually implemented in the following way:

- The values of $\Psi_{i,j}$ and $\theta_{i,j}$ at all nodal points are first set equal to arbitrary initial values, typically the following are used:

$$\Psi_{i,j} = 0$$

$$\theta_{i,j} = 0 \tag{4.10}$$

The assumed θ distribution is that which would exist if there was no convective motion, i.e., if conduction alone existed. Its use is consistent with the assumed distribution of Ψ which implies that there is no flow in the enclosure.

- Eq. (4.7) in conjunction with Eq. (4.8) is used to obtain updated values of $\Psi_{i,j}$. Because iteration is being used, this process should really be repeated over and over until values of $\Psi_{i,j}$ corresponding to the initially assumed distribution of θ are obtained. Experience suggests, however, that it is quite adequate to undertake this step just twice.

- Eq. (4.2) in conjunction with Eq. (4.3) is used to obtain updated values of $\theta_{i,j}$. This step is also undertaken twice.

- Steps (2) and (3) are repeated over and over until convergence is obtained the specified accuracy is | new value of $\Psi_{i,j}$ –old value of $\Psi_{i,j}$ | $\leq 10^{-5}$ in iterative procedures.

- The heat flux rate distribution is obtained by applying Fourier's law at the opposite walls:-

$$q_{w_{1,j}} = \frac{k_a(T_{1,j} - T_{2,j})}{\Delta x}$$

$$q_{w_{M,j}} = \frac{k_a(T_{M-1,j} - T_{M,j})}{\Delta x}$$

(4.11)

- The local Nusselt number is obtained at the boundary conditions in x direction

$$Nu_{1,j} = \frac{1}{\theta_{2,j}}$$

$$Nu_{M,j} = \frac{1}{\theta_{M-1,j}} \frac{q_2}{q_1}$$

(4.12)

where Nu is the local Nusselt number based on W and where it has been noted that

$$\theta_{1,j} = 4 * \theta_{2,j} - \theta_{3,j} + 2 * \frac{\Delta X}{3}, \quad \theta_{M,j} = \frac{q_2}{q_1} * 2 * \Delta X$$

(4.13)

The mean Nusselt numbers are given by:

$$\overline{Nu}_H = \frac{\Delta Y}{A}\left(\frac{Nu_{1,1}}{2} + Nu_{1,2} + Nu_{1,3} + \cdots + Nu_{1,N-1} + \frac{Nu_{1,N}}{2}\right)$$

$$\overline{Nu}_C = \frac{\Delta Y}{A}\left(\frac{Nu_{M,1}}{2} + Nu_{M,2} + Nu_{M,3} + \cdots + Nu_{M,N-1} + \frac{Nu_{M,N}}{2}\right)$$

(4.14)

The finite difference program is found in the appendix.

4.4 Numerical solution justification:

A finite difference numerical procedure is used to solve Eq (3.12) and Eq (3.13). An iterative procedure is used, in which all the variables at the nodal points are first suggested. Then, the updated values are obtained by the governing equations. The process is repeated until the convergence is attained. , the results are obtained for ϕ=-90°, A = 1, For = 0, Ge=0,$Ha^2 = 0$, and $Ra_w = 50$ and the values of the grid size are $\Delta X = \Delta Y = 0.01$, and the total number of points is 30. The grid spacing is found to have no effect on the presented solutions. To check the accuracy of the predicted results, a comparison is done with those of Vasseur et al, for the case of no magnetic field strength with a constant heat flux. The results are shown in Fig. 4.2. It is shown that they are in complete agreement.
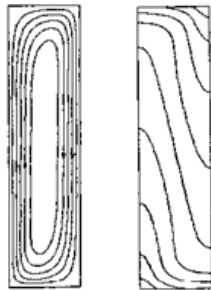
FIG. 10. Streamlines and isotherms for a vertical layer heated from the bottom ($\phi = -\pi/2$) for $A = 4$ and $R = 100$.
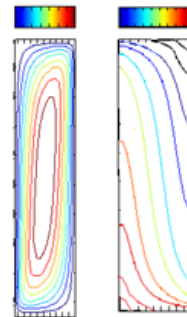
Present Study, stream isothermal for a vertical layer heated from the bottom (ϕ=-90°), A = 4 ,Fr = 0, Ge=0 ,$Ha^2 = 0$, and $Ra_w = 100$.

Fig. 4.2 Predicted results of the streamlines and isotherms for a vertical layer heated from the bottom obtained between the present results and those obtained by Vasseur et al.

By comparison the present results in fig. (4.3-b) to the traditional result in fig. (4.3-a) which are obtained for $Ra_w = 20,100$ and 500, A = 1, For = 0, Ge = 0, $Ha^2 = 0$, it can be seen that the mean Nusselt number have the maximum value at $\phi=135°$ for both results. So, it can found that the results are identical.
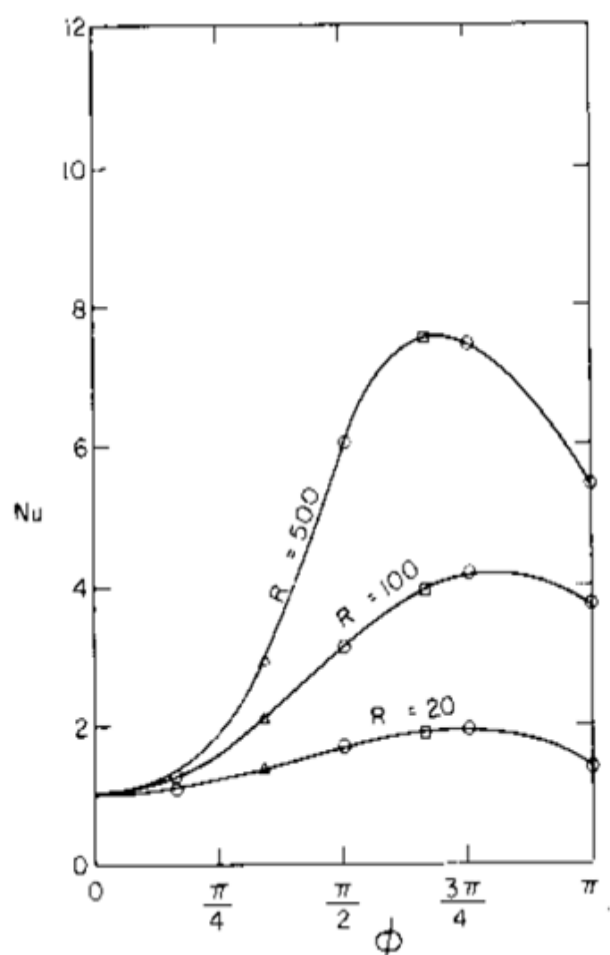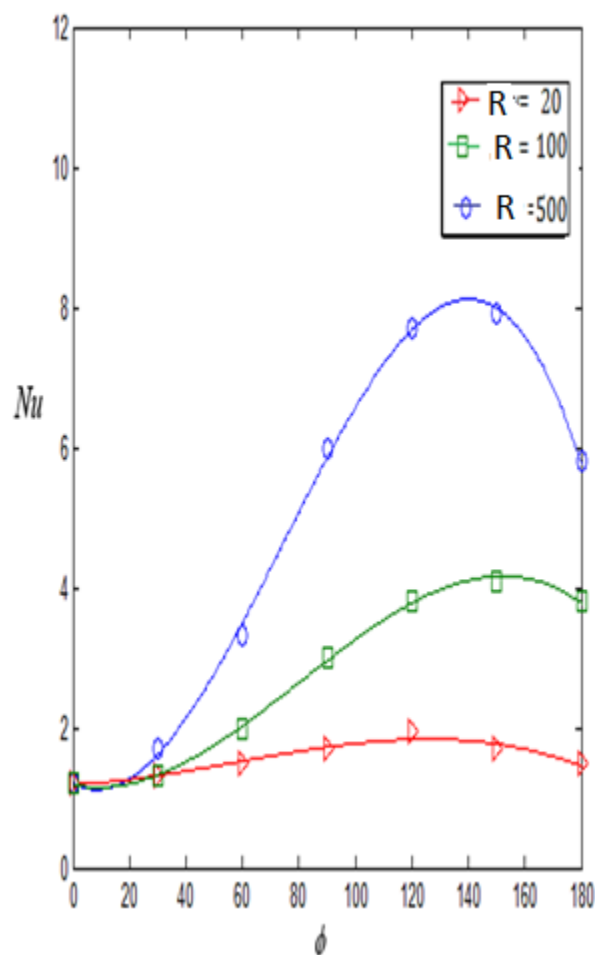
(a) (b)

Fig. 4.3 Variation of mean Nusselt number with Ra_w for various ϕ. (a) Vasseur et al,

(b) Present work

Chapter 5
Results and Discussion

5.1 Introduction:

A numerical study was performed to examine the steady-state, laminar convection iso heat flux problem inside a porous media filled inclined rectangular enclosures, the parameters are the magnetic influence number, the Rayleigh number, the Forchheimer number, the inclination angle, the aspect ratio of the enclosure, and the Gebhart number. Iso-heat flux is applied for heating the two opposing walls of the enclosure while the other two walls are adiabatic. The Finite difference scheme method is used to solve the momentum and energy equations. The effects of all parameters above are included in the final system of partial differential equations and there effects on the fluid flow and temperature are going to be studied. The dimensionless streamlines and isotherms are plotted to obtain flow patterns and temperature fields at different effects of all parameters above. Also, the effects of all parameters on the mean Nusselt number and the center dimensionless stream are plotted.

5.2 The results without viscous and Joule heating effects

5.2.1 Magneto hydrodynamic effects:

The Magneto hydrodynamic effects can be studied by using different values of the magnetic influence number Ha^2 in the momentum equation for $\phi = 30°$, A = 1, Fr = 0.01 and $Ra_w = 100$. The results show that the flow and temperature field are very complex, when the iso-heat flux is applied for heating the two opposing walls of the enclosure while the other two walls are adiabatic.

a. Flow velocity (the dimensionless streamlines)

Fig. 5.1 illustrates the stream function of the numerical results for various Ha^2. AT $Ha^2 = 0$ the q_1 fluid rise up along the left-hand side wall and descends along the center of the enclosure as seen in fluid dimensionless streamlines and the q_2 fluid desends downward along the right-hand side wall and descends along the center of the enclosure quickly due to the usual gravitational buoyancy force, which forms a clockwise flow. At $Ha^2 = 0.03$ and 0.1 the q_1 fluid along the left-hand side wall ascends upward and the q_2 fluid along the right-hand side wall descends downward with smaller dimensionless stream function by comparison with fluid flow at $Ha^2 = 0$.

At $Ha^2 = 3$ and 4 the flow velocity of q_1 fluid near the left-hand side wall has dimensionless streamlines bigger value comparason along the opposite wall. On one hand, with increasing Ha^2, the magnetic force becomes large and the dimensionless stream function of the q_1 fluid along the left-hand side wall has bigger value than the q_2 fluid along the right-hand side wall. On the other hand, the fluid in the middle half enclosure has two circulations of flow with bigger dimensionless stream function value by comparison with the flow along the walls. This is because the magnetic effect is just reversed to the usual gravitational convection effects.
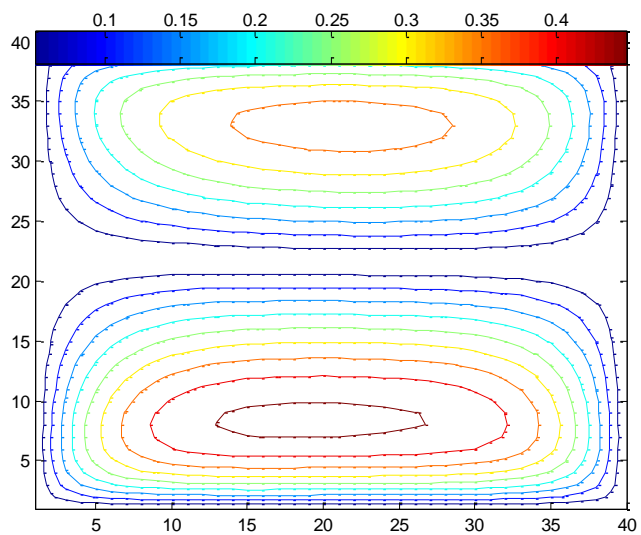
(a)
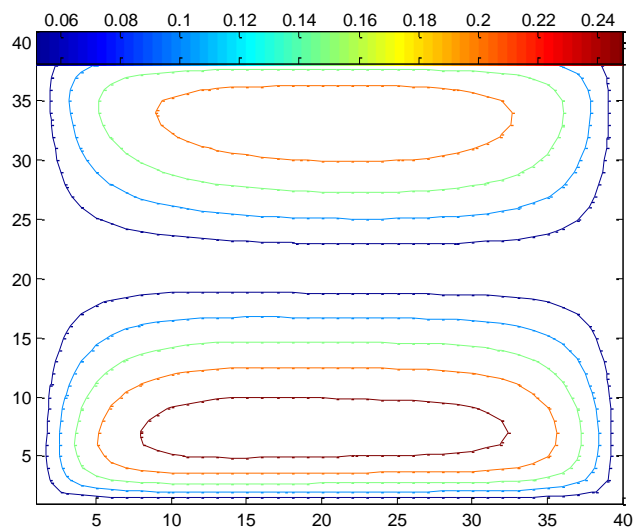
(b)
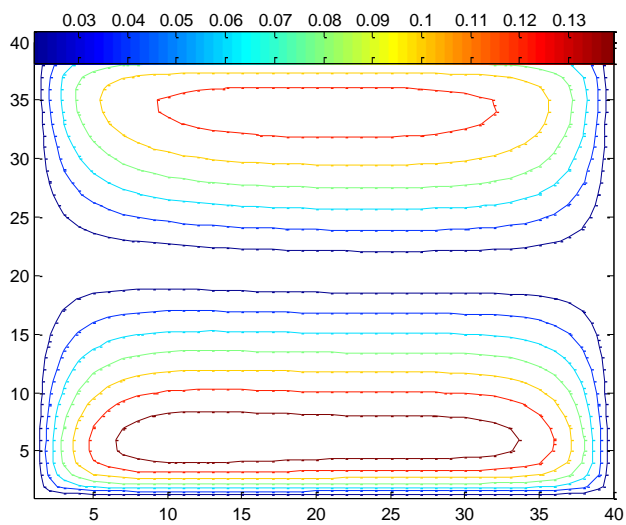
(c)
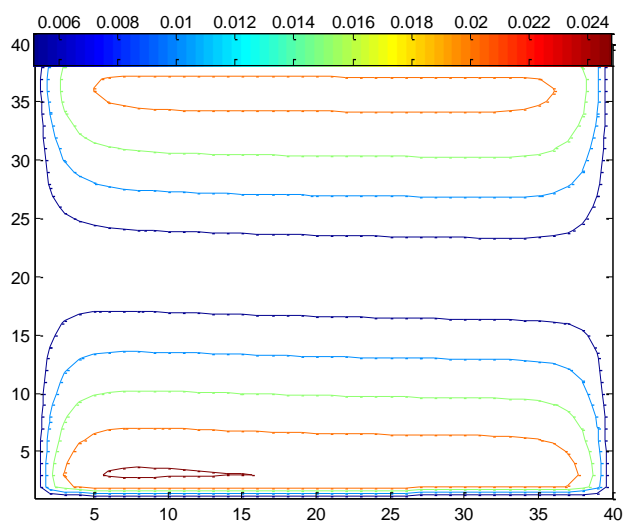
(d)
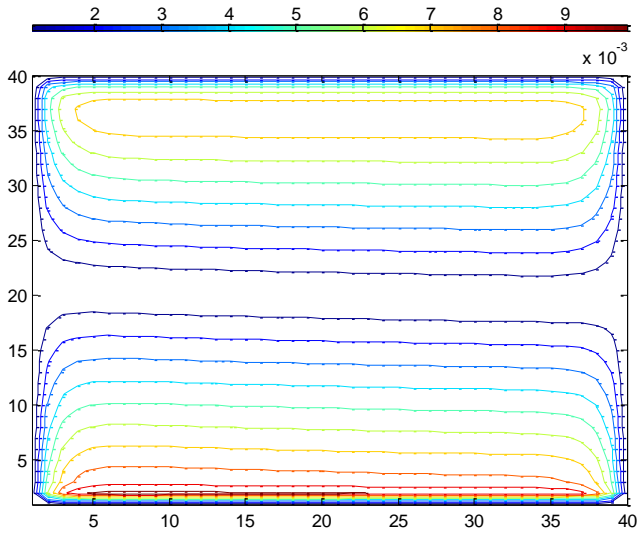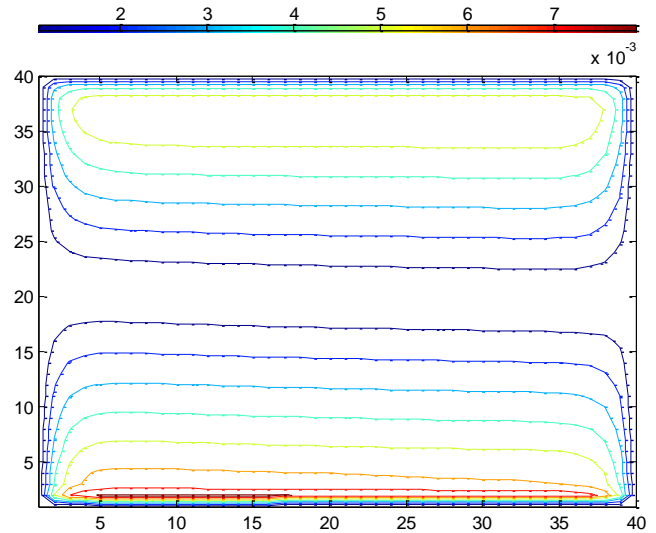
(e)   (f)

Fig. 5.1 Typical dimensionless streamline for various magnetic influence number (a) $Ha^2 = 0$,
(b) $Ha^2 = 0.03$, (c) $Ha^2 = 0.1$, (d) $Ha^2 = 1$, (e) $Ha^2 = 3$, (f) $Ha^2 = 4$ for $\phi = 30°$, A = 1,
For = 0.01, and $Ra_w = 100$

b. Flow temperature (the dimensionless temperature)

Fig. 5.2 illustrates the dimensionless temperature of the numerical results for various $Ha^2 = 0-4$ for $\phi = 30°$, A = 1, For = 0.01, and $Ra_w = 100$, when $Ha^2 = 0$ and 0.03 During convection iso flux dominant heat transfer, the temperature contours with $\theta = 0.22$ occur symmetrically near the opposite side walls of the enclosure. The other temperature contours with $\theta = 0.06$ are symmetrically curves which span the entire enclosure,. At $Ha^2 = 0.1$ the temperature contours increase up to $\theta = 0.25$ near to side walls and $\theta = 0.0.06$ around center of enclosure. From $Ha^2 = 1 - 4$ the temperature contours along the left-hand side wall ascends upward and the fluid along the right-hand side wall descends downward with smaller dimensionless temperature function by comparison with fluid flow at $Ha^2 = 0$.
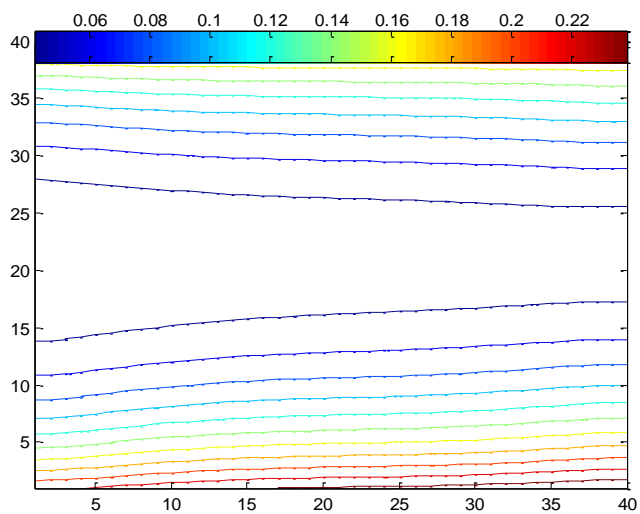
(a)
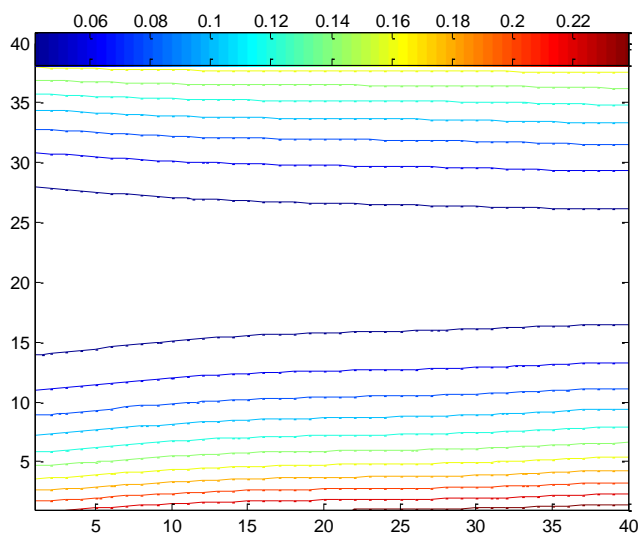
(b)
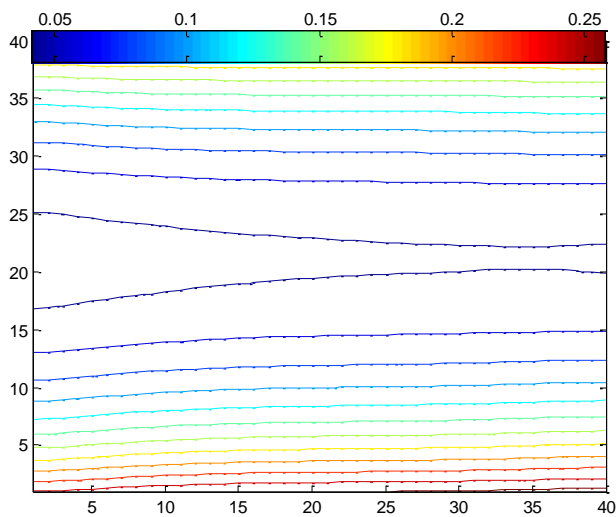
(c)
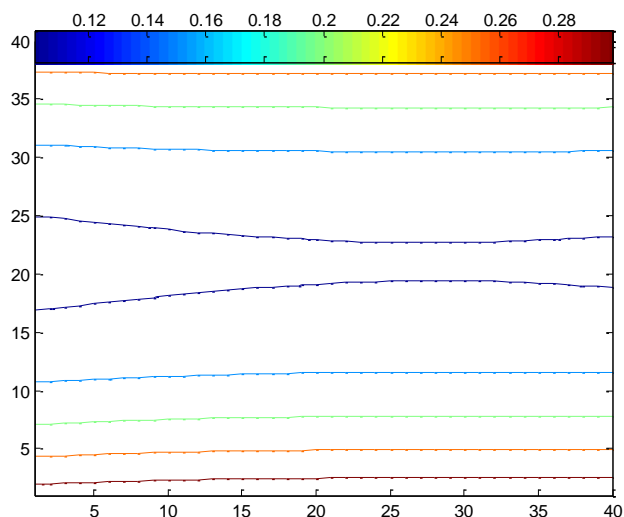
(d)
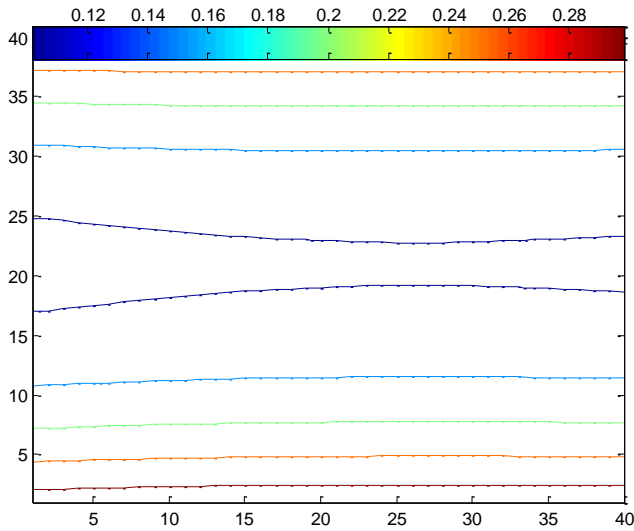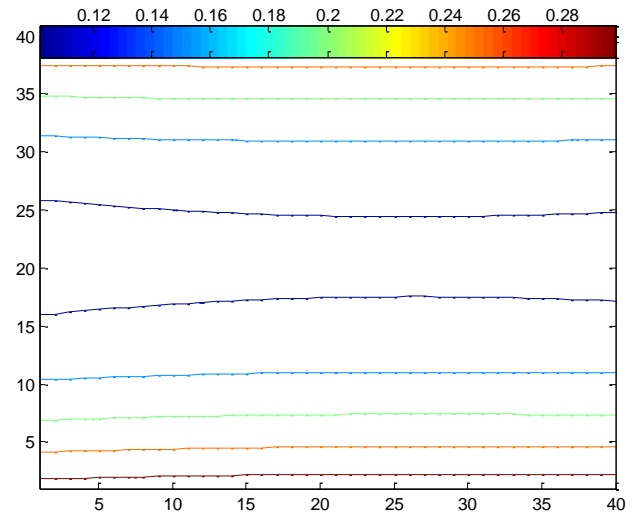
(e)   **(f)**

Fig. 5.2 Typical dimensionless temperature pattern for various magnetic influence number (a) $\text{Ha}^2 = 0$, (b) $\text{Ha}^2 = 0.03$, (c) $\text{Ha}^2 = 0.1$, (d) $\text{Ha}^2 = 1$, (e) $\text{Ha}^2 = 3$, (f) $\text{Ha}^2 = 4$ for ϕ =30°, A = 1, For = 0.01, and $\text{Ra}_w = 100$

c. Nusselt number

Figure (5.3) shows the relation between the variations of mean Nusselt number with magnetic influence number. It can be seen that the mean Nusselt number is decreased by increasing the magnetic influence number; this is due to decreasing in dimensionless temperature form along the left-hand to the upper half region and the lower half region along the right-hand side wall. This is due to the retarding effects of magneto hydrodynamic forces.
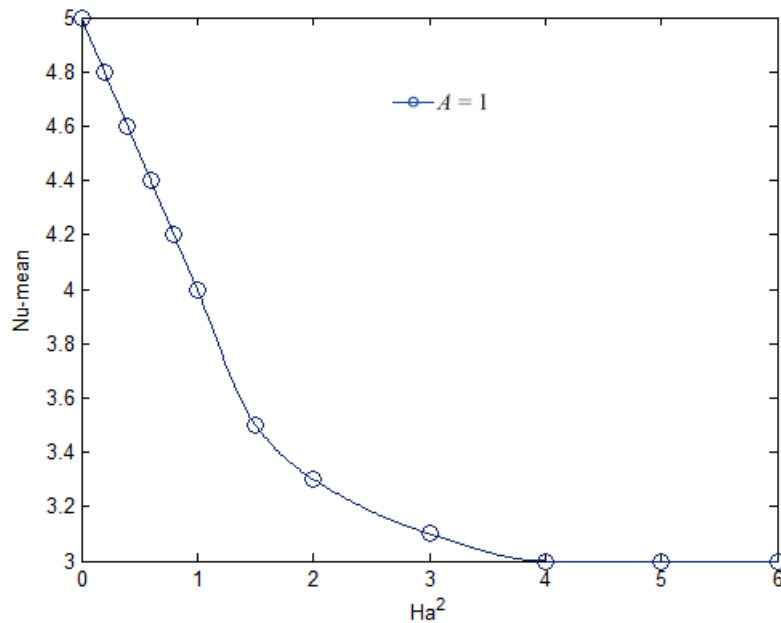
Fig. 5.3 Variation of Nu-mean with Ha^2 for an enclosure for ϕ =30°,

A = 1, For = 0.01, and Ra$_w$ = 100

5.2.2 The Modified Rayleigh number effects:

a. Flow velocity (the dimensionless streamlines)

Figure (5.4) illustrates the stream function of the numerical results for various Ra$_w$,for ϕ =30°, A = 1, For = 0.01, and Ha^2 = 0.02, when the iso-heat flux is applied for heating opposing walls of the enclosure while the other two walls are adiabatic. When the Rayleigh number is small, i.e. At Ra$_w$ = 1 the hot fluid along the left-hand side wall and the cold fluid along the right-hand side wall have small values of the dimensionless stream function of the fluid flow, which is 0.003 at the center of the upper side and the lower side of the enclosure. However, when Raw is

100, the magnetic force has large effect on the heat flux rate, and the value of the dimensionless

stream line becomes 0.55 at Ha^2=0.002 at the center of the enclosure.

(a)

(b)

(c)
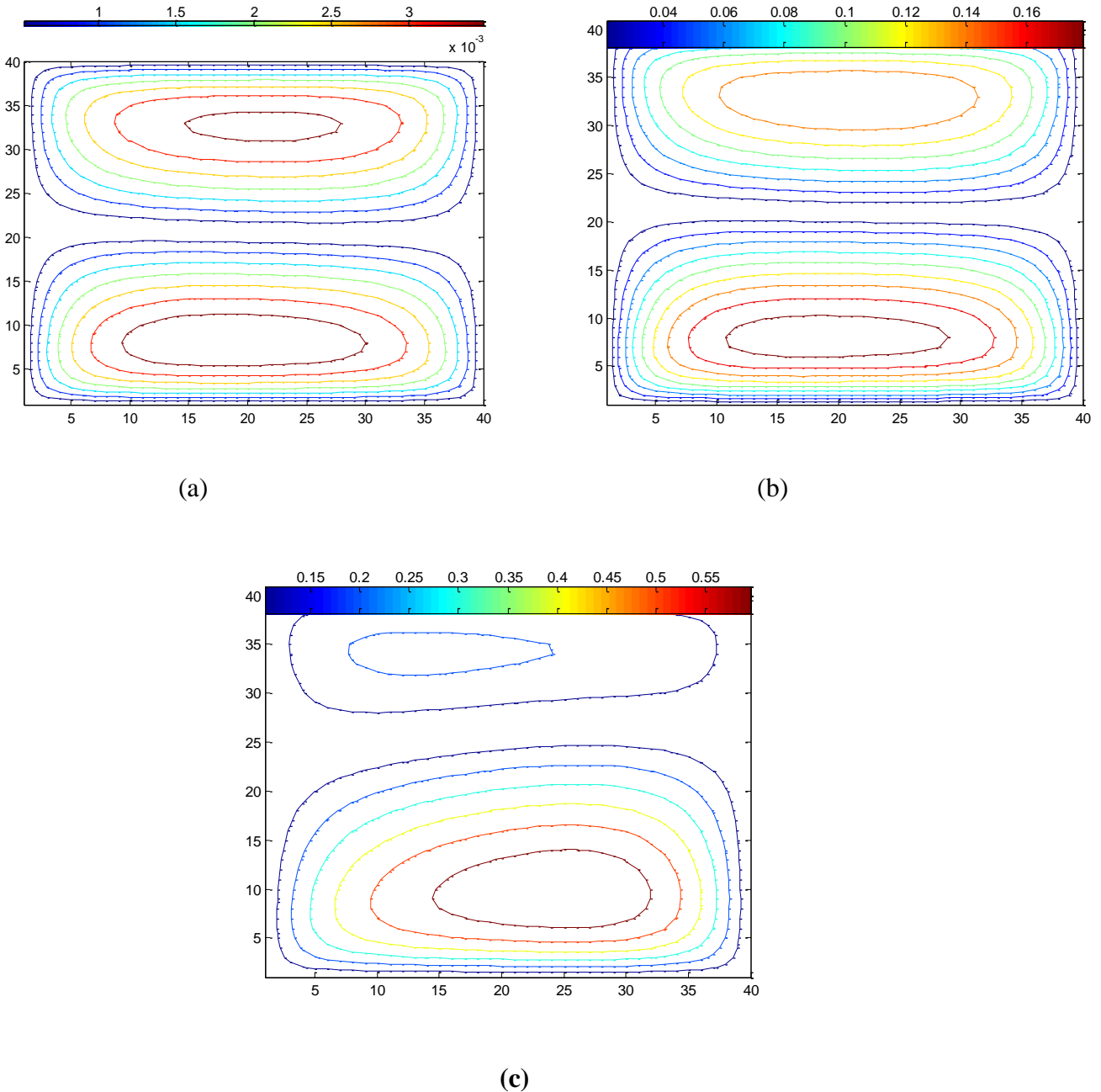
Fig. 5.4 Typical dimensionless streamline patterns for various Darcy-modified Rayleigh number
(a) Ra$_w$ = 1, (b) Ra$_w$ = 50, (c) Ra$_w$ = 100, for ϕ =30°, A = 1, For = 0.01, and Ha^2 = 0.02
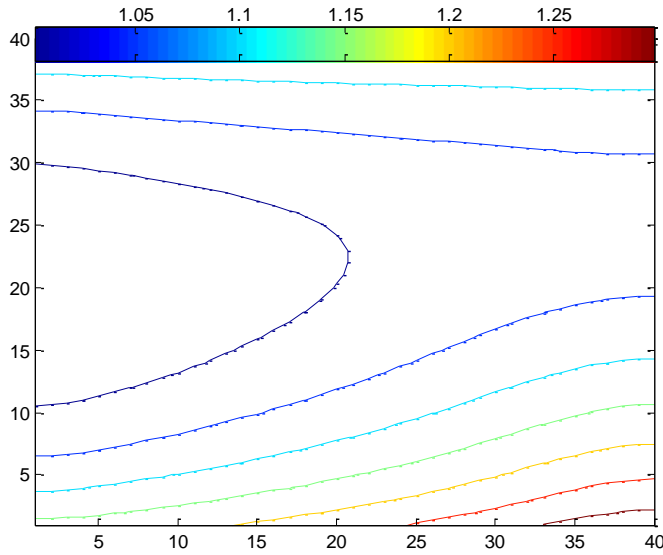
b. Flow temperature (the dimensionless temperature)

Fig. 5.5 illustrates the dimensionless temperature of the numerical results for various Ra_w , for ϕ =30°, A = 1, For = 0.01, and $Ha^2 = 0.02$.when Ra_w =1 the dimensionless temperature of the q_1 fluid in the left -hand side wall and the right-hand side wall of the enclosure is increased up to 0.25.when Ra_w =100 the dimensionless temperature of the q_1 fluid in the lower right-hand corner of the enclosure is increased up to 1.25.
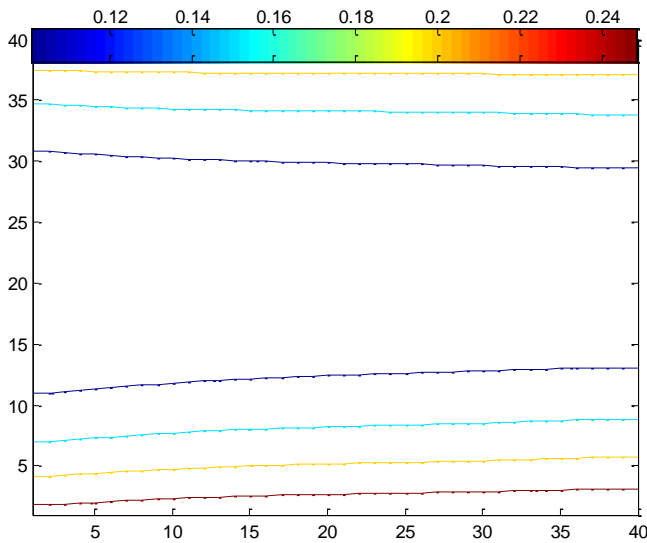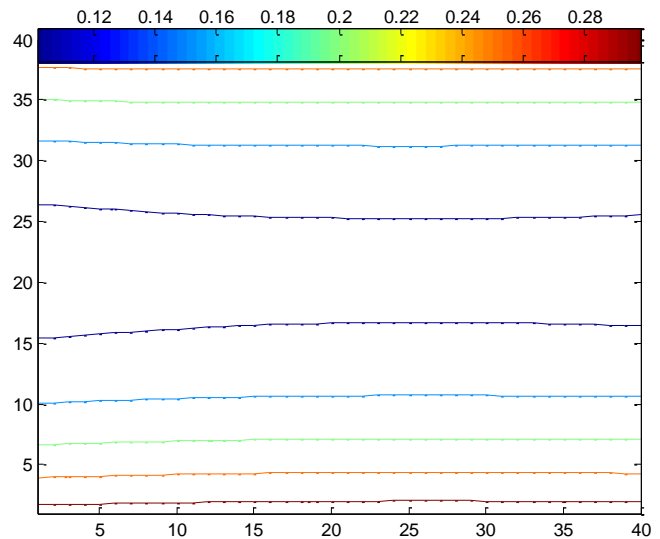
(a)   (b)

(c)

Fig. 5.5 Typical dimensionless temperature patterns for various Darcy-modified Rayleigh number (a) $Ra_w = 1$, (b) $Ra_w = 50$, (c) $Ra_w = 100$, for $\phi = 30°$, A = 1, For = 0.01, and $Ha^2 = 0.02$

c. Nusselt number

The effect of the aspect ratio A of the enclosure on the mean Nusselt number, It is found that, the increasing of aspect ratio A=1, 3 and 5 the Nusselt number decreases; this is due to larger thermal resistance in the heat transfer direction. It is clear also in this figure the favorable buoyancy forces effect in defining fluid velocities and higher coefficients of heat transfer.

It can be seen also, the mean Nusselt number is increased to reach the maximum value at $Ra_w =$ 100; this is due to increasing in convection heat flux when the Modified Rayleigh number is increased.
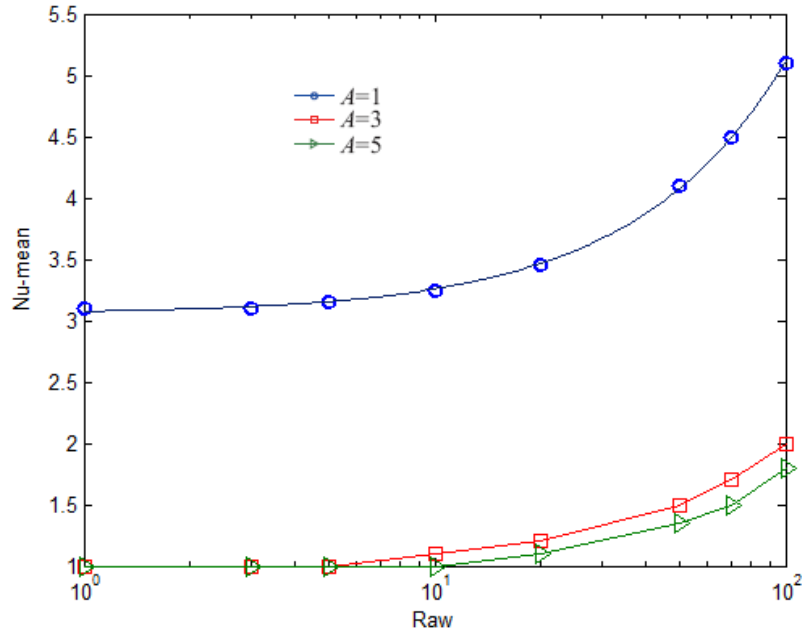
Fig. 5.6 Variation of Nu-mean with Raw for an enclosure for various A for $\phi =30°$,

For = 0.01, and $Ha^2 = 0.02$

5.2.3 The inclination angle of the enclosure effects:

In order to examine the effects of the inclination angle, computations are carried out for a fluid with ϕ varying from 0 ° to 180 °. Numerical results are obtained for Ra_w = 100, A = 1, Ha^2 = 0.02, and For = 0.01.

a. Flow velocity (the dimensionless streamlines)

Figure (5.7) illustrates the effect of the inclination angle of the enclosure on the dimensionless streamlines with other parameters unchanged, as it is shown, ϕ has a certain effect on the heat flux and fluid flow. When ϕ = 0 the q_1 fluid along the left-hand side wall descends downward and the q_2 fluid along the right-hand side wall ascends upward due to buoyancy forces, which forms a counterclockwise flow When ϕ = 90, the q_1 fluid along the left-hand side wall ascends upward and the q_2 fluid along the right-hand side wall descends downward which forms a clockwise flow. When ϕ = 180, the magnitude of magnetic force has no effect on the heat flux rate, this is due to the location of the q1 wall which becomes at the upper portion of the enclosure. The Maximum heat transfer rates are obtained for inclination angels nearly 60°.

(a)   (b)
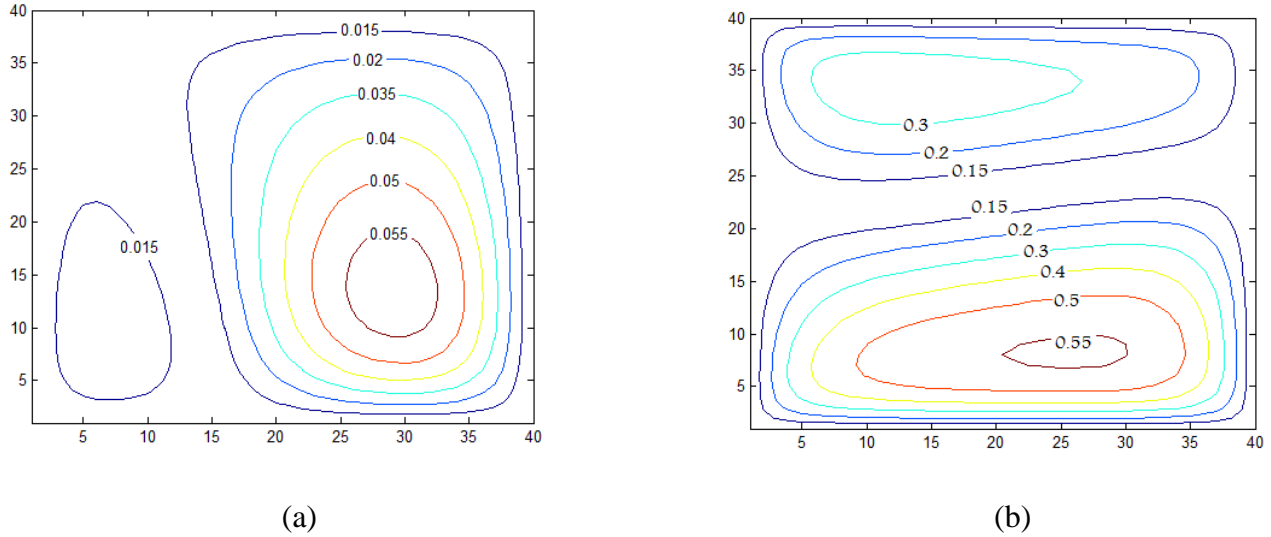
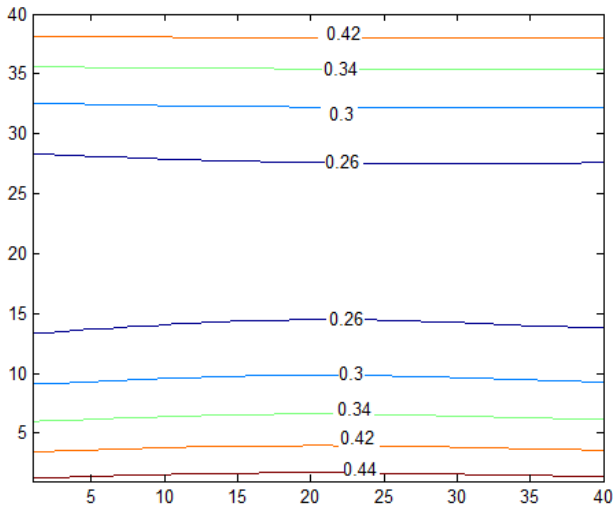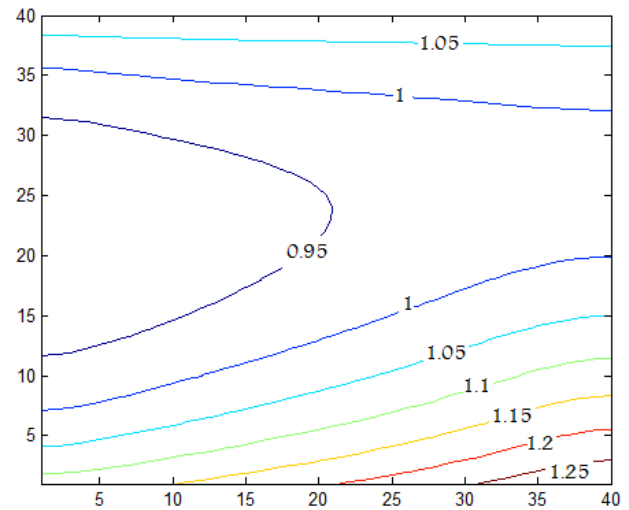Fig. 5.7 Typical dimensionless streamline patterns for various inclination angle of the enclosure
(a) $\phi = 0$, (b) $\phi = 90°$ for $Ra_w = 100$, A = 1, For = 0.01, and $Ha^2 = 0.02$

b. Flow temperature (the dimensionless temperature)

Fig. 5.8 illustrates the effect of the inclination angle of the enclosure on the dimensionless temperature with other parameters unchanged of the numerical results for various $\phi = 0°, 90°$. During convection iso flux dominant heat transfer, when $\phi = 0°$ the temperature contours with $\theta = 0.44$ occur near along left hand side wall of the, and along right side wall of enclosure with $\theta = 0.42$ and the other temperature contours with $\theta = 0.26$ which is spanned in the entire enclosure, when $\phi = 90°$ the dimensionless temperature value increases for the q_1 fluid in the lower right-hand corner of the enclosure, it becomes larger than 1.25.

(a)   (b)

Fig. 5.8Typical dimensionless temperature patterns for various inclination angle of the enclosure
(a) $\phi = 0$, (b) $\phi = 90°$ for $\text{Ra}_w = 100$, A = 1, For = 0.01, and $\text{Ha}^2 = 0.02$

c. Nusselt number

Figures (5.9 and 5.10) show the mean Nusselt number and dimensionless center-stream function
have maximum value are obtained for inclination angels nearly $60°$. On the other hand, it can be
seen that the dimensionless center-stream function is decreased by increasing the magnetic
influence number and it is increased by increasing the Rayleigh number.
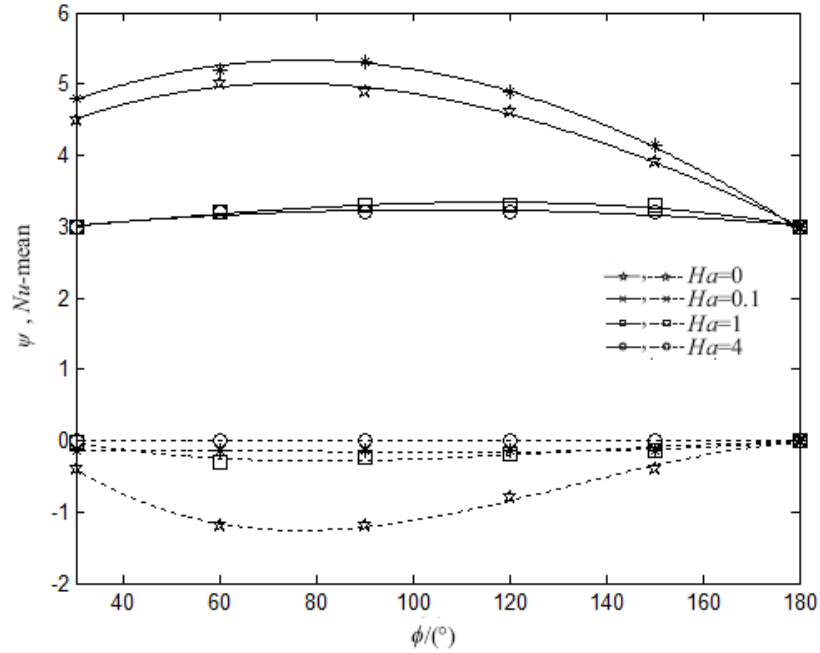
Fig. 5.9 Variation of mean Nusselt number and dimensionless center-stream function with angle of inclination for an enclosure for various Ha^2 for $Ra_w = 100$, A = 1, For = 0.01
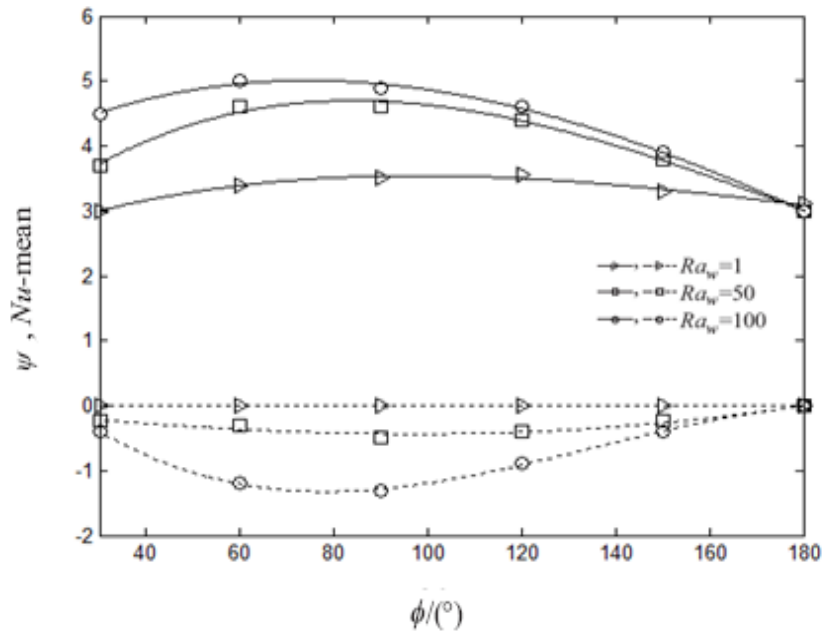
Fig. 5.10 Variation of mean Nusselt number and dimensionless center-stream function with angle of inclination for an enclosure for various Ra_w for A = 1, For = 0.01, and $Ha^2 = 0.02$

5.3 The results with viscous and Joule heating effects:

5.3.1 Magneto hydrodynamic effects:

The Magneto hydrodynamic effects can be studied by using different values of the magnetic influence number Ha^2 in the momentum equation for $\phi = 30°$, A = 1, Fr = 0.01, Ge = 0.05 and $Ra_w = 100$. The results show that the flow and temperature field are very complex, when the iso-heat flux is applied for heating the two opposing walls of the enclosure while the other two walls are adiabatic.

a. Flow velocity (the dimensionless streamlines)

Fig. 5.11 illustrates the stream function of the numerical results for various Ha^2 , the fluid circulation is strongly dependent on Magneto hydrodynamic as we have seen in Fig. 5.1. At $Ha^2 = 0$ the dimensionless stream function of the q_1 fluid along the left-hand side wall has bigger value than the q_2 fluid along the right-hand side wall which is 1.5. At $Ha^2 = 0.03$ and 0.1 the hot fluid along the left-hand side wall ascends upward and the cold fluid along the right-hand side wall descends downward with smaller dimensionless stream function by comparison with fluid flow when $Ha^2 = 0$. When $Ha^2 = 3$ and 4 the q_1 fluid in left-hand side wall has dimensionless stream bigger value than the opposite wall. On the other hand, the fluid in the middle half enclosure has two circulations of flow and by increasing Ha^2 the circulation of flow
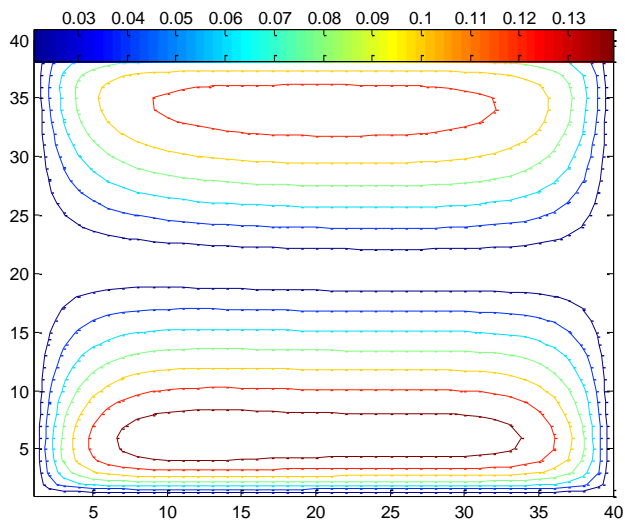
becomes along the left-hand side wall and the dimensionless stream function is decreased to reach negligible value at $Ha^2 = 4$.
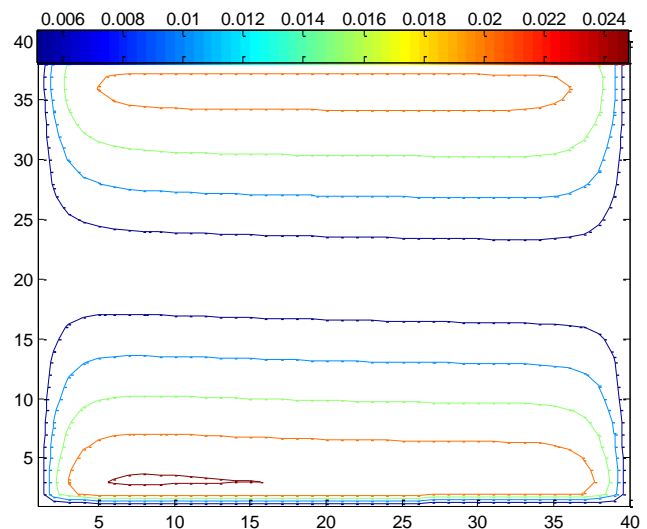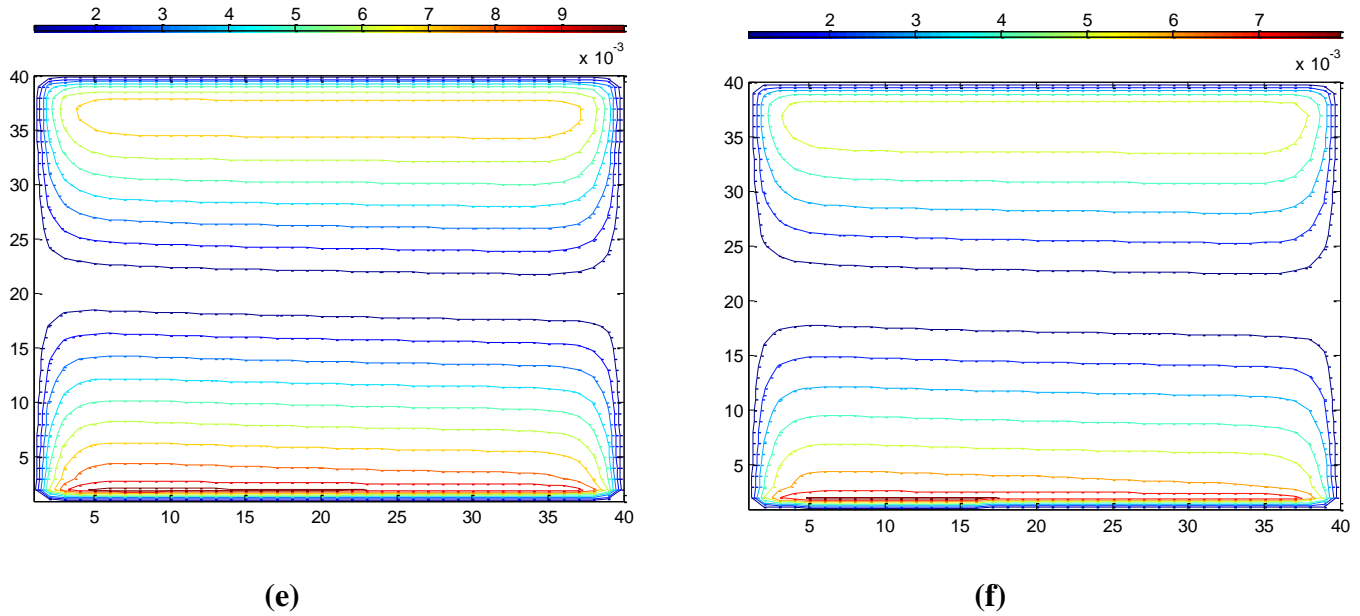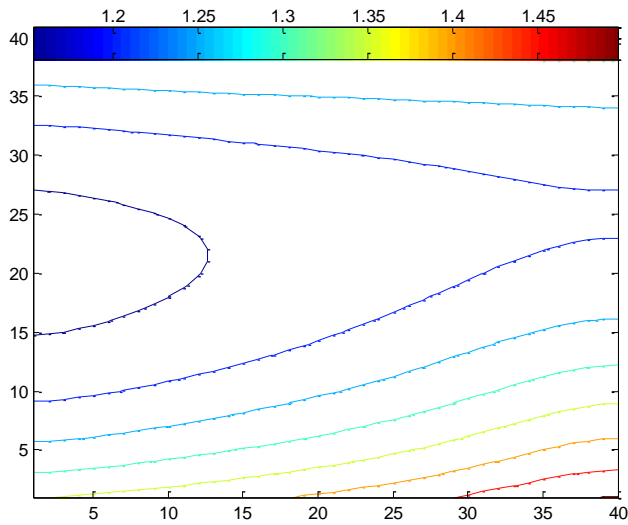

(a)

(b)

(c)

(d)

(e)

(f)
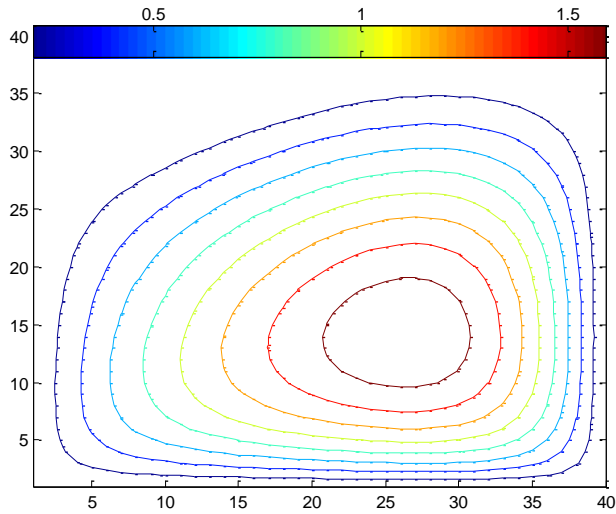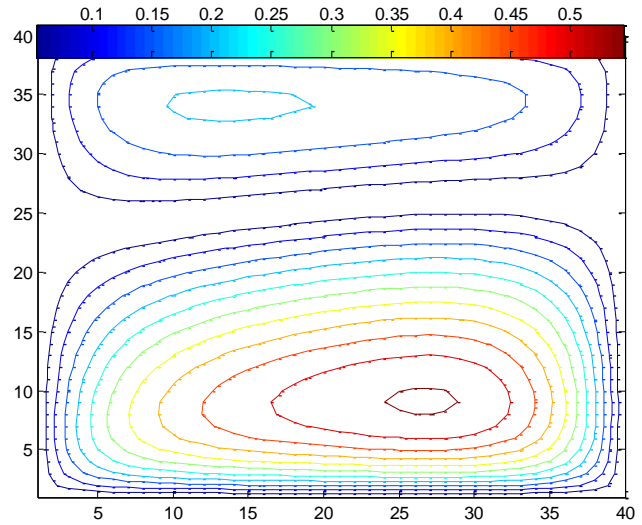
Fig. 5.11 Typical dimensionless streamline patterns for various magnetic influence number (a) $Ha^2 = 0$, (b) $Ha^2 = 0.03$, (c) $Ha^2 = 0.1$, (d) $Ha^2 = 1$, (e) $Ha^2 = 3$, (f) $Ha^2 = 4$ for $\phi = 30°$, $A = 1$, For $= 0.01$, Ge $= 0.05$ and $Ra_w = 100$
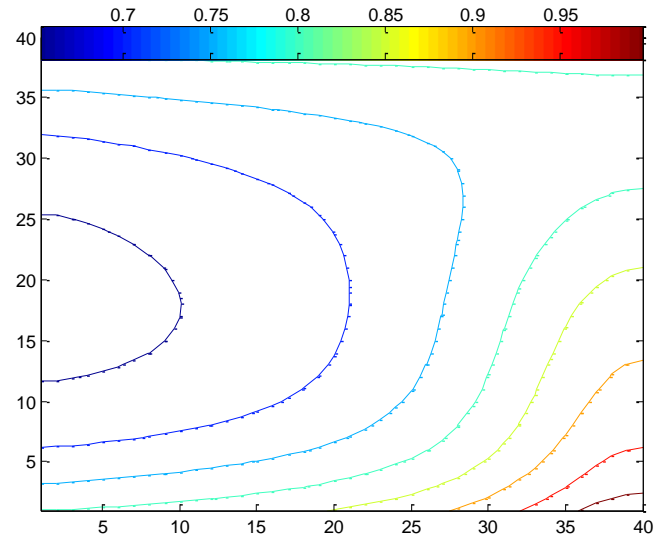
b. Flow temperature (the dimensionless temperature)

Figure 5.12 illustrate the dimensionless temperature of the numerical results for various Ha^2. At $Ha^2 = 0$ the dimensionless temperature value is increased for the q_1 fluid in the lower right -hand corner of the enclosure to become larger than 1.45 due to the Gebhart number effects in Joule term as seen in fluid isothermal contours. When $Ha^2 = 0.03$ the q_1 fluid isothermal along the left-hand side wall ascends upward and the q_2 fluid along the right-hand side wall descends downward with smaller dimensionless stream function by comparison with fluid flow at $Ha^2 =$

0. On the other hand, from Ha^2= 1- 4 the temperature contours with Θ=0.28 occur symmetrically near the side walls of the enclosure the other temperature contours with Θ=0.12 are symmetrically curves which span the entire enclosure.
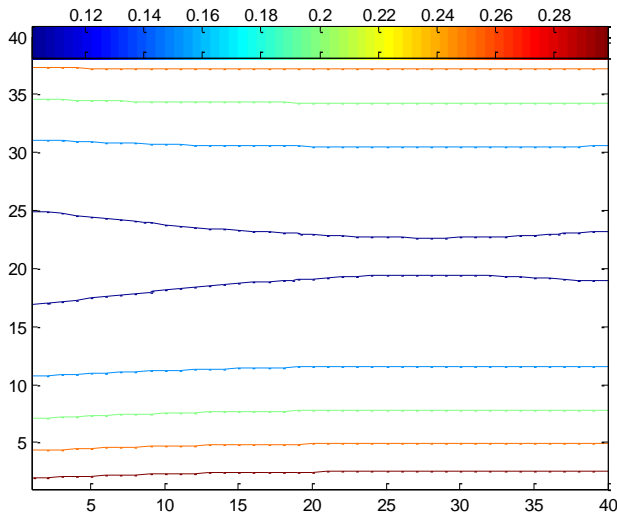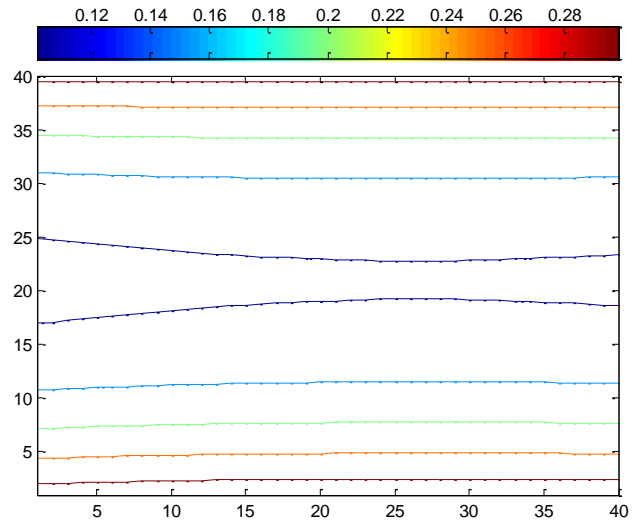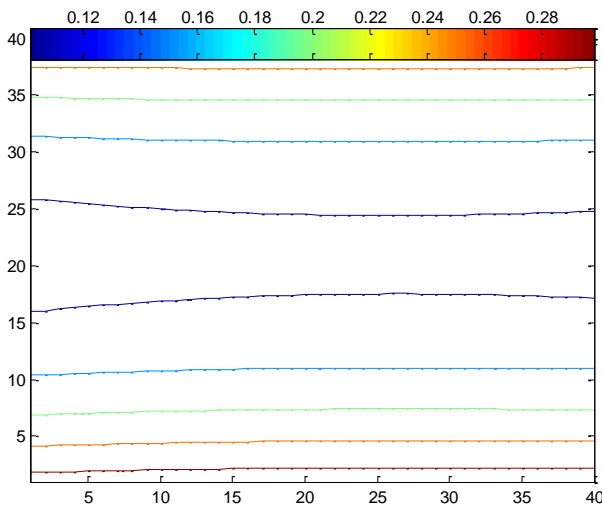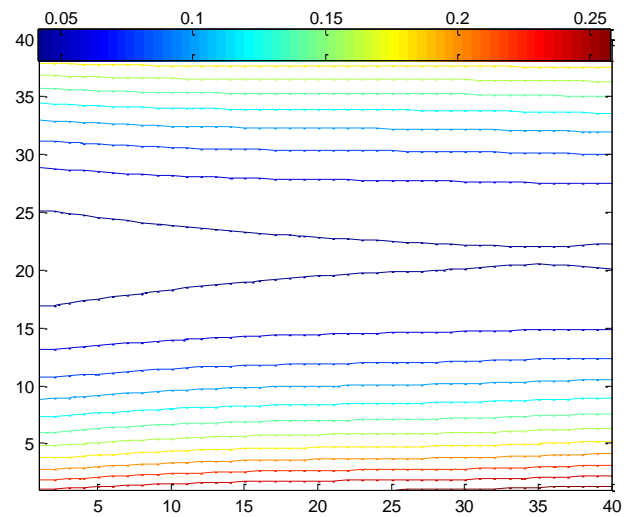

(a)   (b)

(c)

(d)

(e)

(f)

Fig. 5.12 Typical dimensionless temperature patterns for various magnetic influence number (a) Ha² = 0, (b) Ha² = 0.03, (c) Ha² = 0.1, (d) Ha² = 1, (e) Ha ² = 3, (f) Ha² = 4 for ϕ =30°, A = 1, For = 0.01, Ge = 0.05 and Ra$_w$ = 100

c. Nusselt number

Figure (5.13) shows the relation between the variations of mean Nusselt number with magnetic influence number. It can be seen that the mean Nusselt number is decreased by increasing the magnetic influence number; due to decreasing in the dimensionless temperature value in the lower half region along the left-hand side wall.
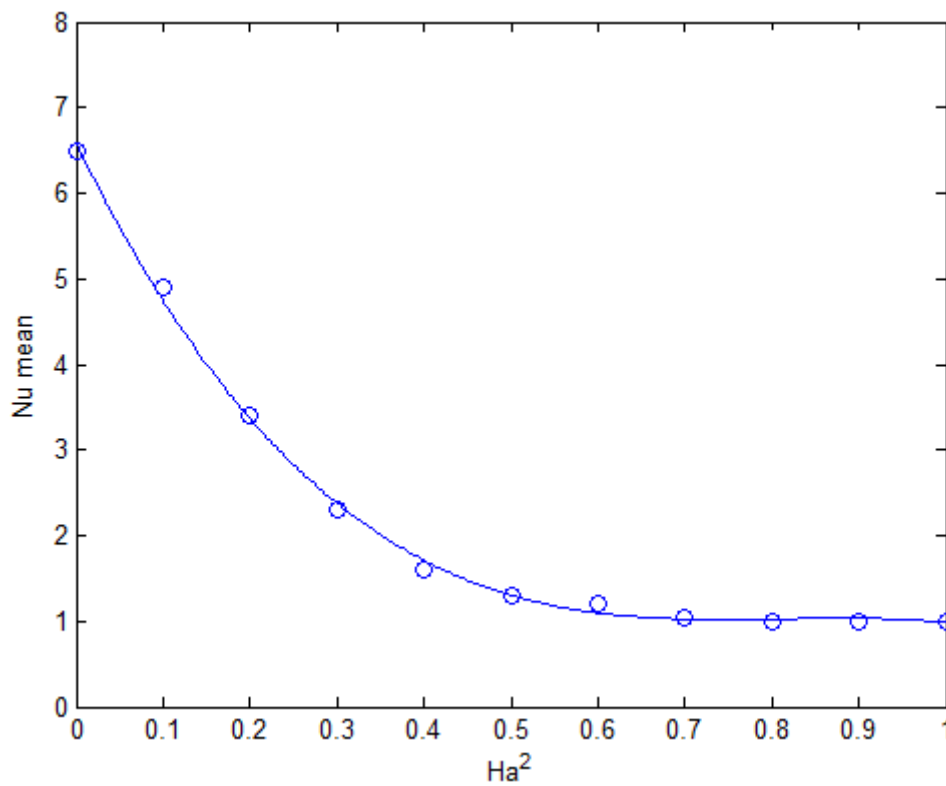

Fig. 5.13 Variation of Nu-mean with Ha^2 for an enclosure for $\phi = 30°$, A = 1, For = 0.01,
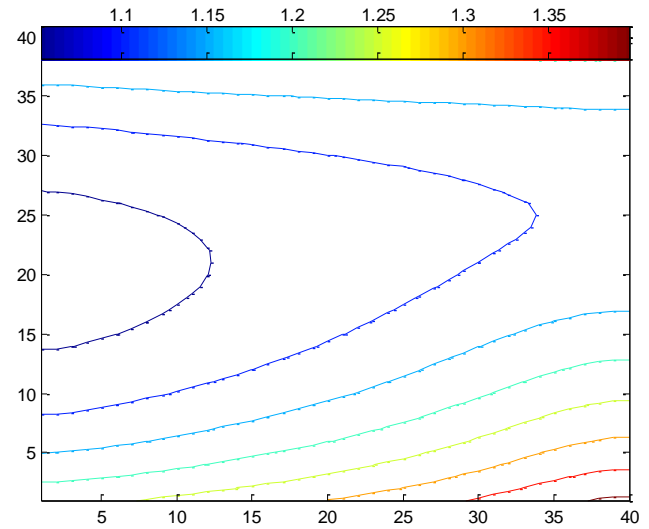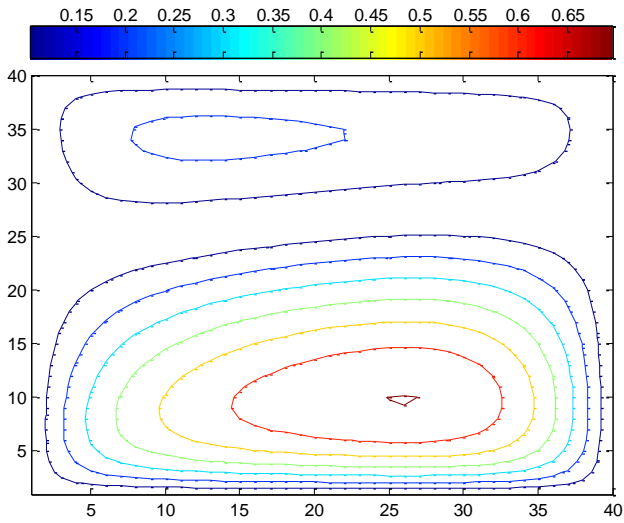
Ge = 0.05 and $Ra_w = 100$

5.3.2 The Gebhart number effects:

Figure (5.14) illustrates the effect of Gebhart number on the dimensionless streamlines and isotherms patterns with other parameters unchanged, as it is shown, By increasing the Gebhart number the dimensionless temperature value is increased therefore, the fluid velocity is increased At Ge = 0 the q_1 fluid rises up along the left-hand side hot wall and the q_2 fluid descends along the right-hand side cold wall as seen in fluid isothermal contours. On the other hand, the fluid is rotating around the centre of the enclosure with maximum fluid flow by comparison with the flow along the walls. From Ge = 0.02-0.05 the dimensionless temperature of the q_1 fluid in the lower right-hand corner of the enclosure is increased and the q_2 fluid in the upper left -hand corner of the enclosure is decreased, therefore, the mean Nusselt number at the hand side wall is decreased.

By increasing Ge the dimensionless stream lines are moved to the upper right-hand corner and the dimensionless temperature value is increased for the q_1 fluid in the lower right -hand corner of the enclosure to become larger than 1.75 at Ge = 0.08; this is due to the increasing in the work done by magnetic field force on the fluid and the increasing in the friction between the fluid layers inside the enclosure. Figure (5.15) shows the relation between the variations of mean Nusselt number at the cold-hand side wall with Gebhart number. It can be seen that the mean Nusselt number is decreased by increasing in the Gebhart number. This is due to the excessive heating of the conductive fluid layers and consequently small temperature gradients between the walls and the surfaces.
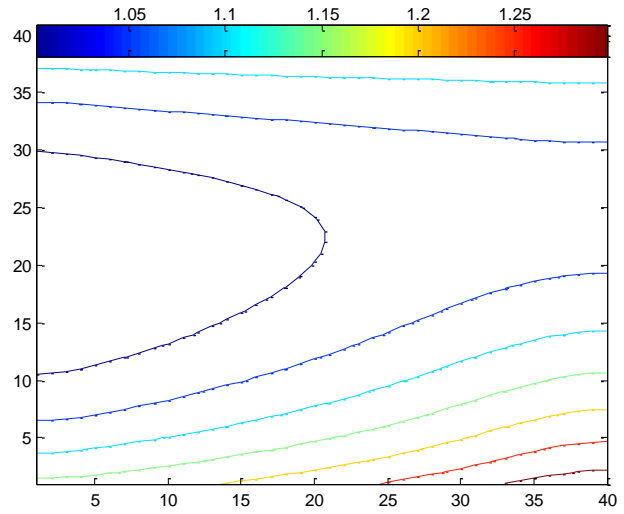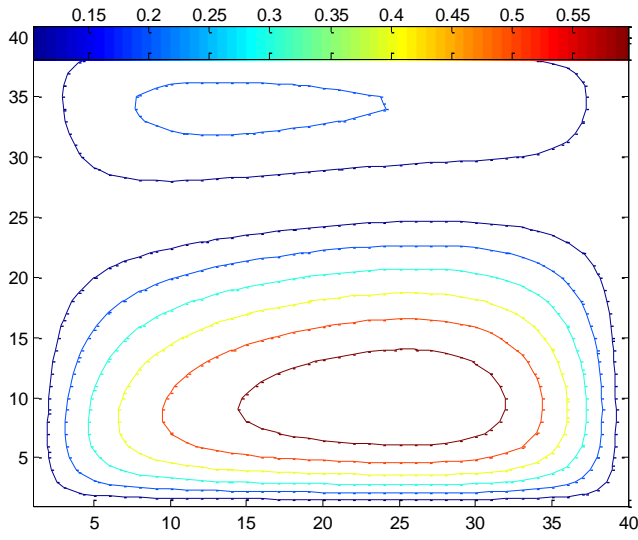
(a)

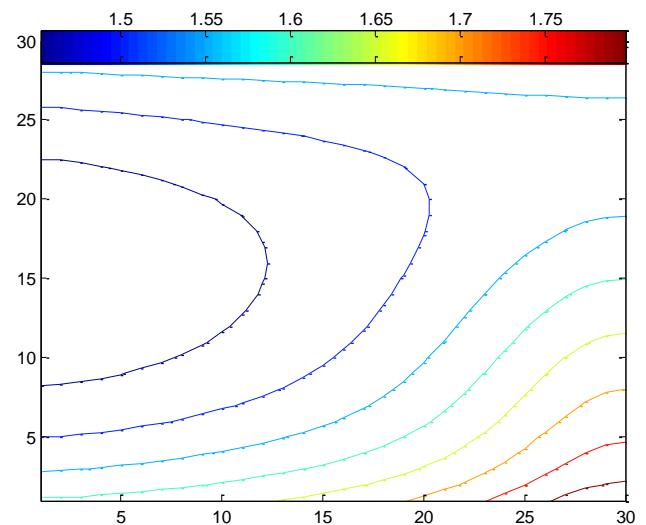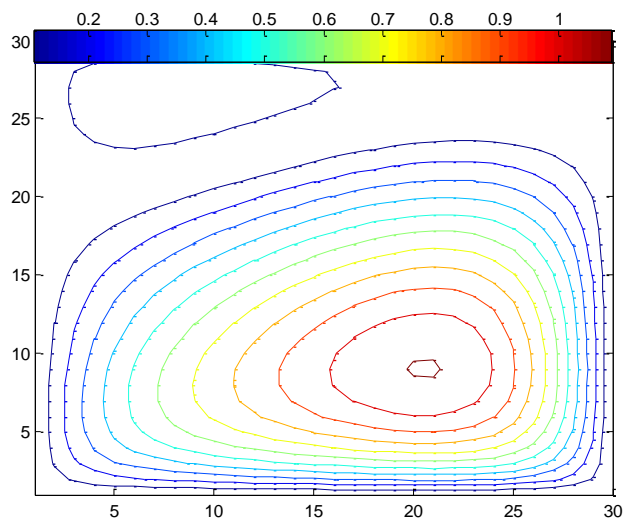(b)
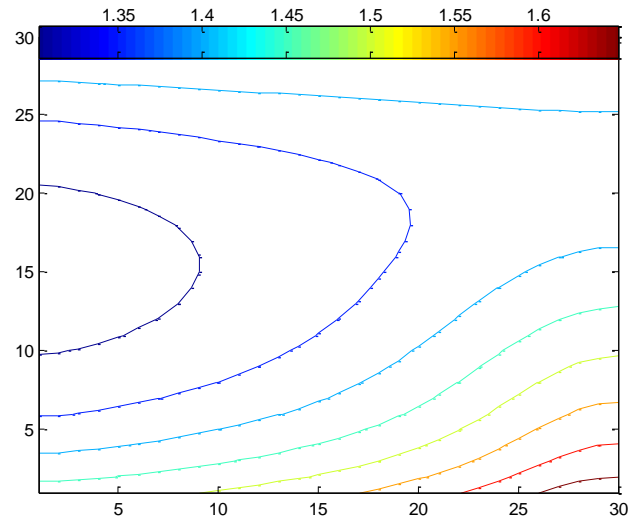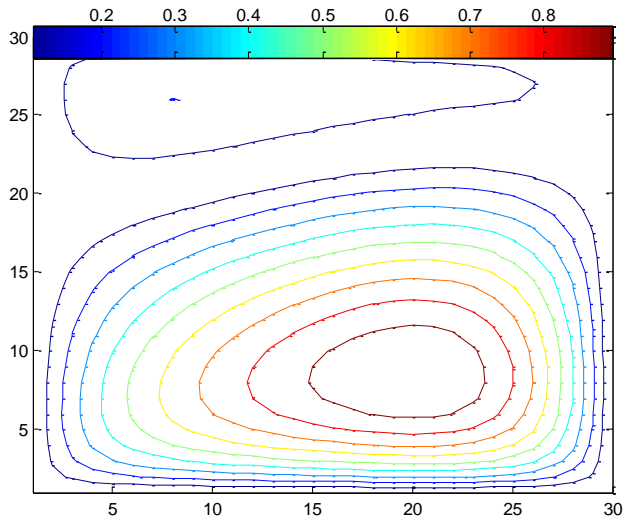
(c)

(d)

Fig. 5.14 Typical dimensionless streamline and dimensionless temperature patterns for various Gebhart number (a) Ge = 0, (b) Ge = 0.02, (c) Ge = 0.05, (d) Ge = 0.08 for ϕ =30°, Ha^2 = 0.02, A = 1, For = 0.01, and Ra_w = 100
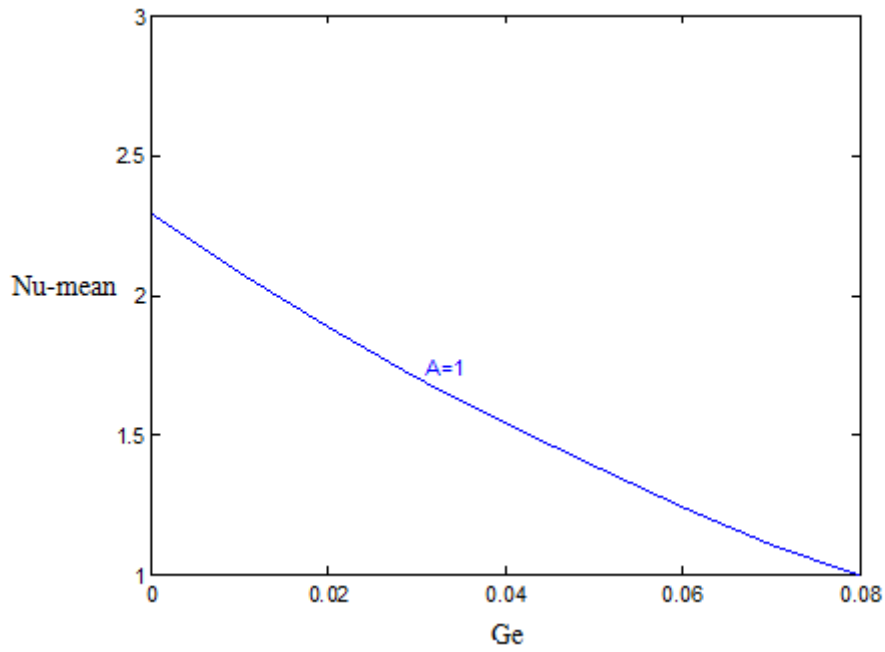
Fig. 5.15 Variation of Nu-mean at the cold-side wall with Ge for an enclosure for

$\phi = 30°$, $Ha^2 = 0.02$, A = 1, For = 0.01, and $Ra_w = 100$

5.3.3 Modified Rayleigh number effects:

a. Flow velocity (the dimensionless streamlines)

Figure (5.16) illustrates the effect of Rayleigh number in the momentum equation on the dimensionless streamlines with other parameters unchanged, as it is shown, Rayleigh number has a certain effect on the heat flux and fluid flow. When the Rayleigh number is small, the magnitude of magnetic force has little effect on the heat transfer rate. At Ra_w = 1 the hot fluid along the left-hand side wall and the cold fluid along the right-hand side wall have small value of dimensionless stream function of fluid flow, which is 0.004 at the centre of the enclosure. By increasing Ra_w to reach the maximum value which is 100, the magnetic force has larger effect on the heat flux rate and the value of dimensionless stream line reaches to become 0.8 at $Ha^2 = 0.02$ at the centre of the enclosure.
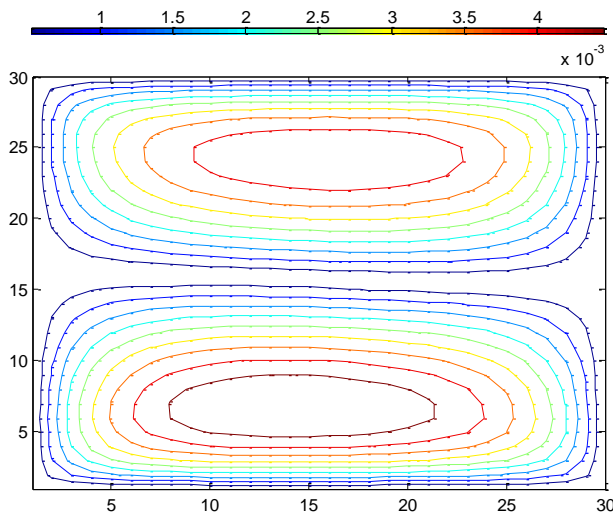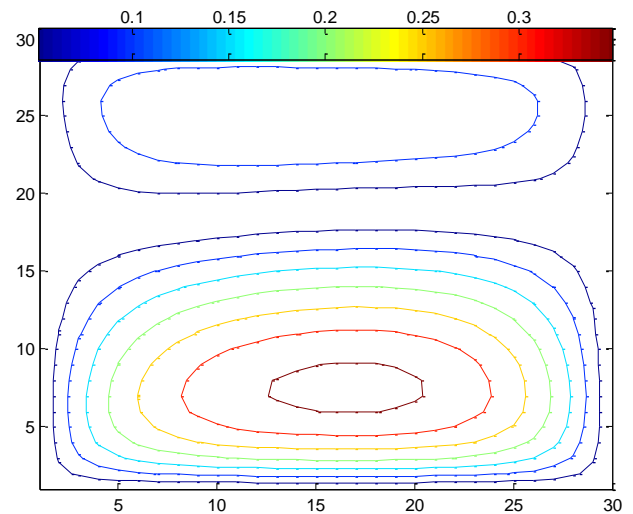
(a)   (b)
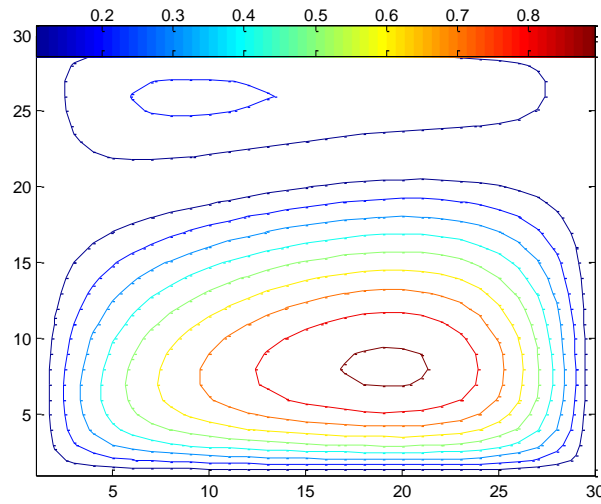
(c)

Fig. 5.16 Typical dimensionless streamline patterns for various Darcy-modified Rayleigh number (a) $Ra_w = 1$, (b) $Ra_w = 50$, (c) $Ra_w = 100$, for $\phi = 30°$, A = 1, For = 0.01, Ge=0.05, and $Ha^2 = 0.02$

b. Flow temperature (the dimensionless temperature)

Fig. 5.17 illustrates the dimensionless temperature of the numerical results for various Ra_w. During convection iso flux dominant heat transfer, the temperature contours with $\theta = 0.38$ occur symmetrically near the side walls of the enclosure and the other temperature contours with $\theta = 0.22$ are symmetrically curves which span the entire enclosure, when $Ra_w = 100$ the dimensionless temperature of the q_1 fluid in the lower right-hand corner of the enclosure increases, and the q_2 fluid in the upper left-hand corner of the enclosure decreases.
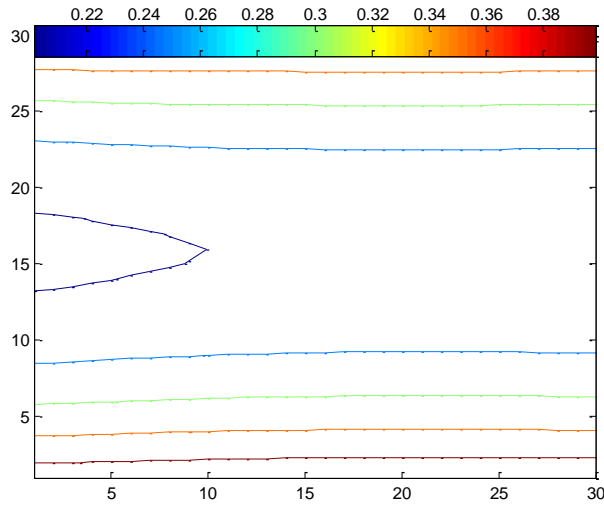
(a)

(b)
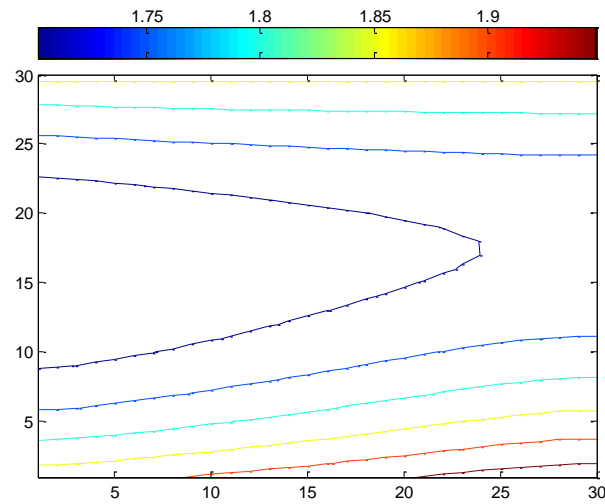
(c)

Fig. 5.17 Typical dimensionless temperature patterns for various Darcy-modified Rayleigh number (a) $Ra_w = 1$, (b) $Ra_w = 50$, (c) $Ra_w = 100$, for $\phi = 30°$, A = 1, For = 0.01, Ge=0.05, and $Ha^2 = 0.02$

c. Nusselt number
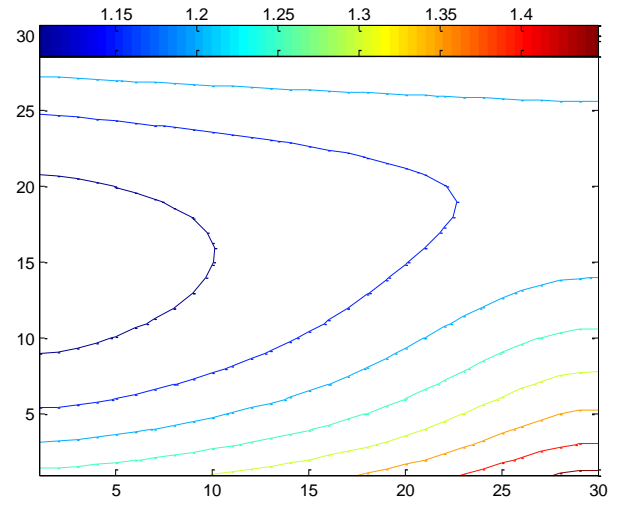
The values of the mean Nusselt number are shown in Fig. (5.18). It is clear that as Ra_w

increases, Nu-mean increases. This is due to favorable buoyancy forces. It is found that,

When the Rayleigh number is small, the value of mean Nusselt number is 1 and then

increases to reach the maximum value at $Ra_w = 100$. It can be seen that the variation of

Nu-mean with Ra_w for an enclosure for various A, as it is shown, the maximum value of

mean Nusselt number is at A=1, this is due to negligible convection heat transfer effects

when $Ra_w \to 0$ and the value of Nu-mean = 1 means a pure conduction .
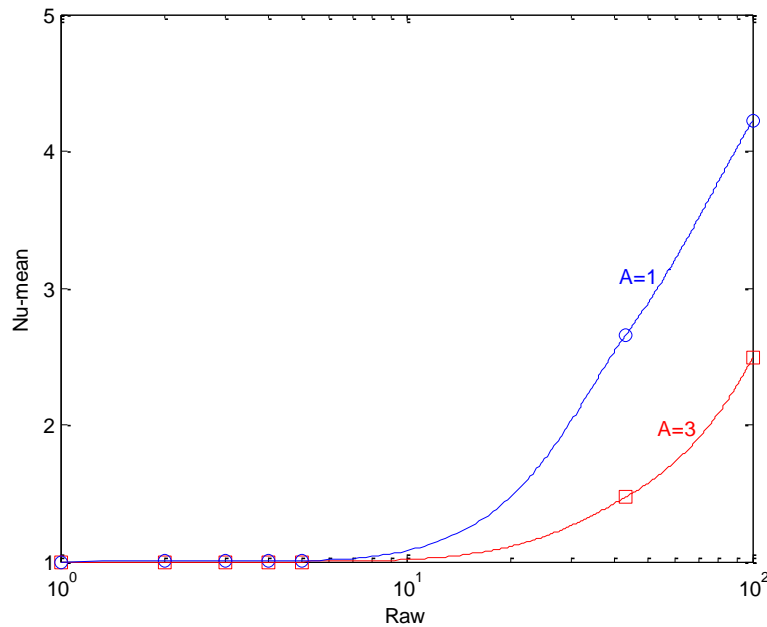
Fig. 5.18 Variation of Nu-mean with Ra_w for an enclosure for various A for ϕ =30°,

A = 1, Fr = 0.01, Ge=0.05, and $Ha^2 = 0.02$

5.3.4 The inclination angle of the enclosure effects:

In order to examine the effects of the inclination angle, computations are carried out for a fluid with ϕ varying from 0 ° to 180 °. Numerical results are obtained for Ra_w = 100, A = 1, Ha^2 = 0.02, For = 0.01 and Ge=0.05.

a. Flow velocity (the dimensionless streamlines)

Figure (5.19) illustrates when $\phi = 0$ the hotter fluid along the left-hand side wall descends downward, and the fluid along the right-hand side wall ascends upward due to the usual gravitational buoyancy force, which forms a counterclockwise flow, which forms a counterclockwise flow. When $\phi = 90$, the q_1 fluid along the left-hand side wall ascends upward and the q_2 fluid along the right-hand side wall descends downward with bigger value than dimensionless streamlines when $\phi = 0$, which forms a clockwise flow. When $\phi = 180$, the magnitude of magnetic force has no effect on the heat flux rate, this is due to the location of the q1 wall which becomes at the upper portion of the enclosure. The Maximum heat transfer rates are obtained for inclination angels nearly 60°.

(a)   (b)

Fig. 5.19 Typical dimensionless streamline patterns for various inclination angle of the enclosure (a) $\phi = 0$, (b) $\phi = 90°$ for $Ra_w = 100$, A = 1, For = 0.01, Ge=0.05, and $Ha^2 = 0.02$

b. Flow temperature (the dimensionless temperature)

Fig. 5.20 illustrates the dimensionless temperature of the numerical results for various $\phi = 0°, 90°$ for $Ra_w = 100$, A = 1, For = 0.01, $Ha^2 = 0.02$ and Ge = 0. 05. During convection iso flux dominant heat transfer, when $\phi = 0$ ° the temperature contours with $\theta = 0.08$ occur near along left hand side wall of the, and along right side wall of enclosure with $\theta = 0.02$, when $\phi = 90$ ° the dimensionless temperature value increases for the hot fluid in the left-hand wall of the enclosure, it becomes larger than 0.18.
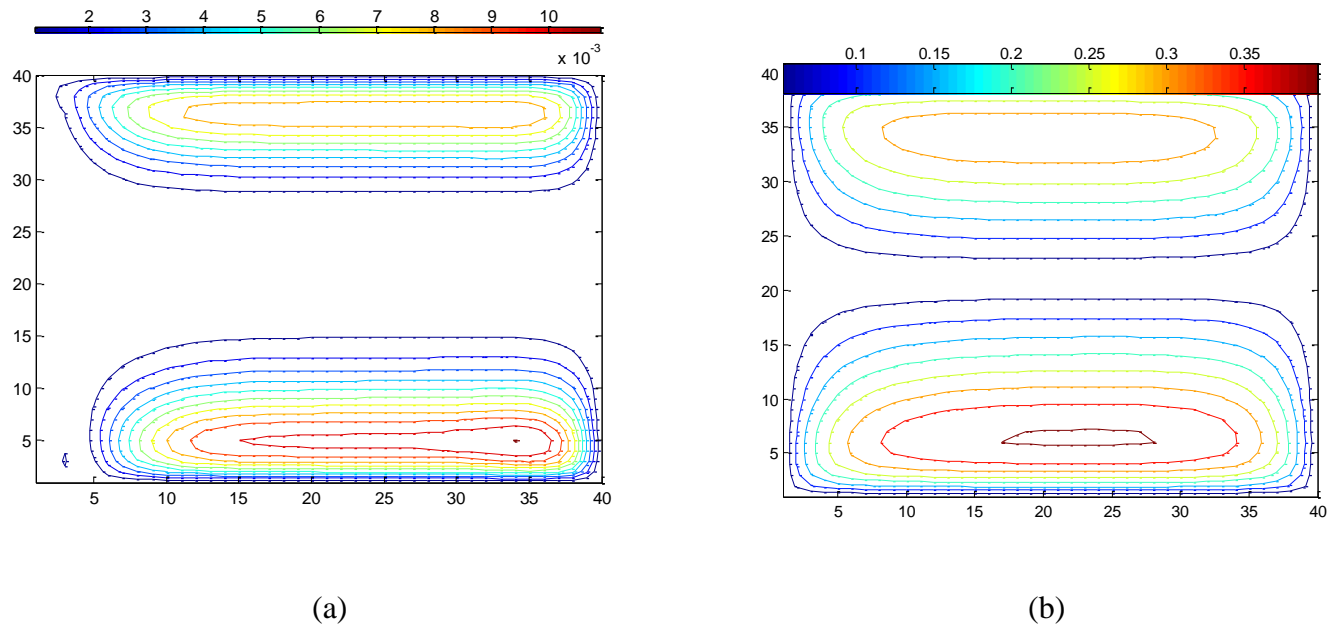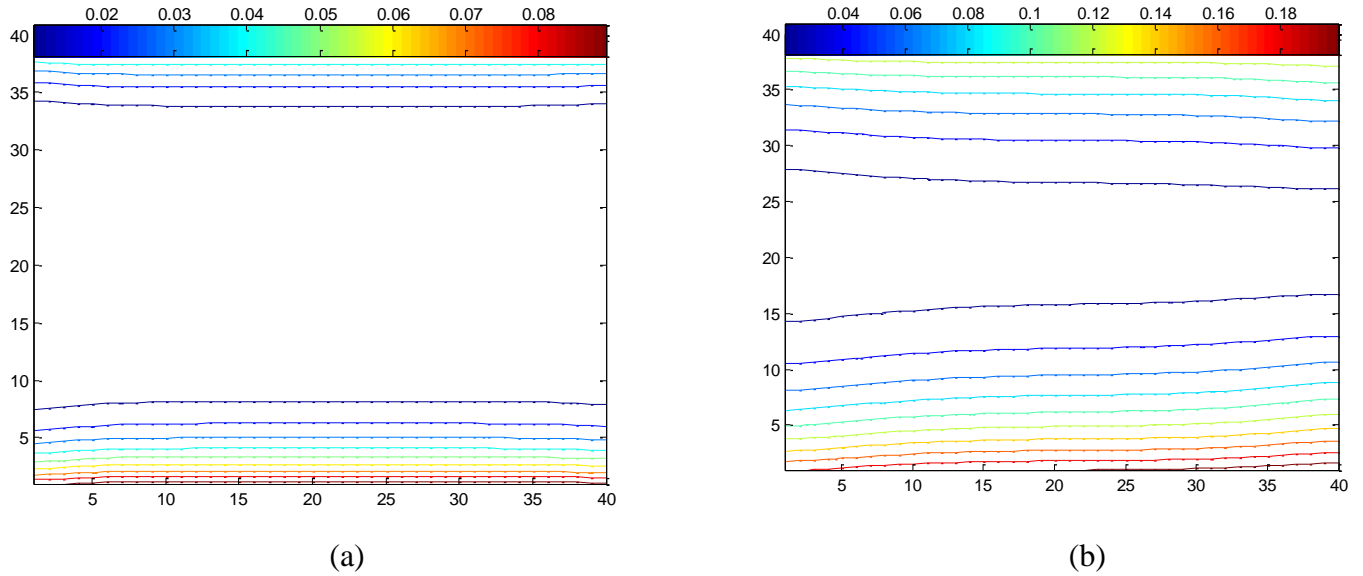
Fig. 5.20 Typical dimensionless temperature patterns for various inclination angle of the enclosure (a) $\phi = 0$, (b) $\phi = 90°$ for $Ra_w = 100$, A = 1, For = 0.01, Ge=0.05, and $Ha^2 = 0.02$

c. Nusselt number

Figures (5.21, 5.22, and 5.23) show the relation between the variation of mean Nusselt number and dimensionless center-stream function with angle of inclination for an enclosure for various Ha^2, Ra_w, and Ge, respectively. It can be seen that the mean Nusselt number and dimensionless center-stream function have maximum value are obtained for inclination angels nearly $60°$. On the other hand, it can be seen that the dimensionless center-stream function is decreased by increasing in the magnetic

influence number and it is increased by increasing the modified Rayleigh number; this is

due retardation effect of the magnetic field and favorable effect of the buoyancy forces.

Fig. 5.21 Variation of mean Nusselt number and dimensionless center-stream function with angle of inclination for an enclosure for various Ha^2 for $Ra_w = 100$, A = 1, For = 0.01, and Ge=0.05
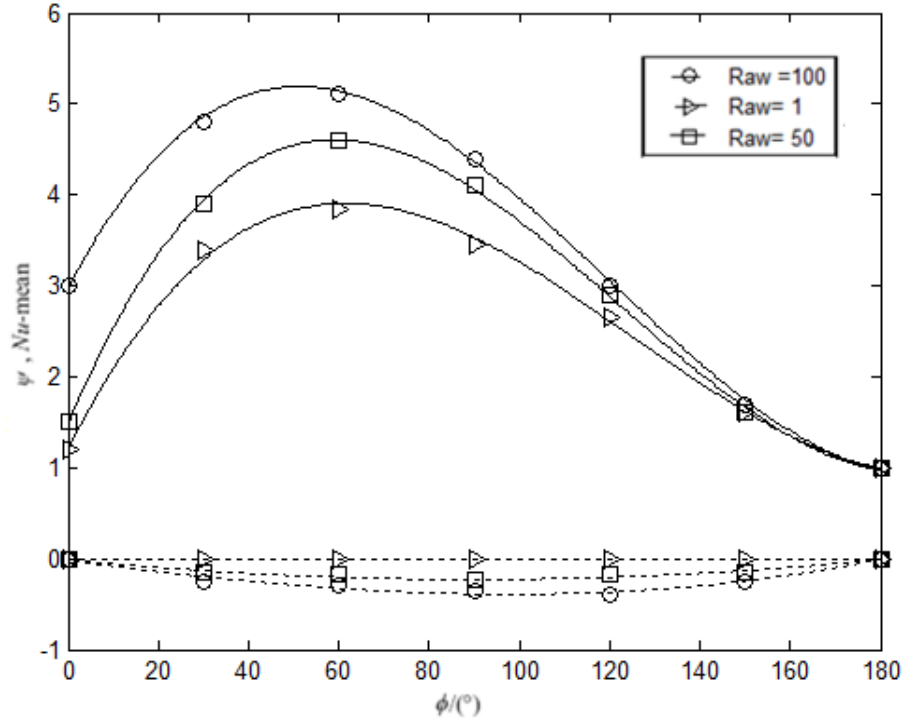
Fig. 5.22 Variation of mean Nusselt number and dimensionless center-stream function with angle of inclination for an enclosure for various Ra_w for A = 1, For = 0.01, Ge=0.05, and $Ha^2 = 0.02$

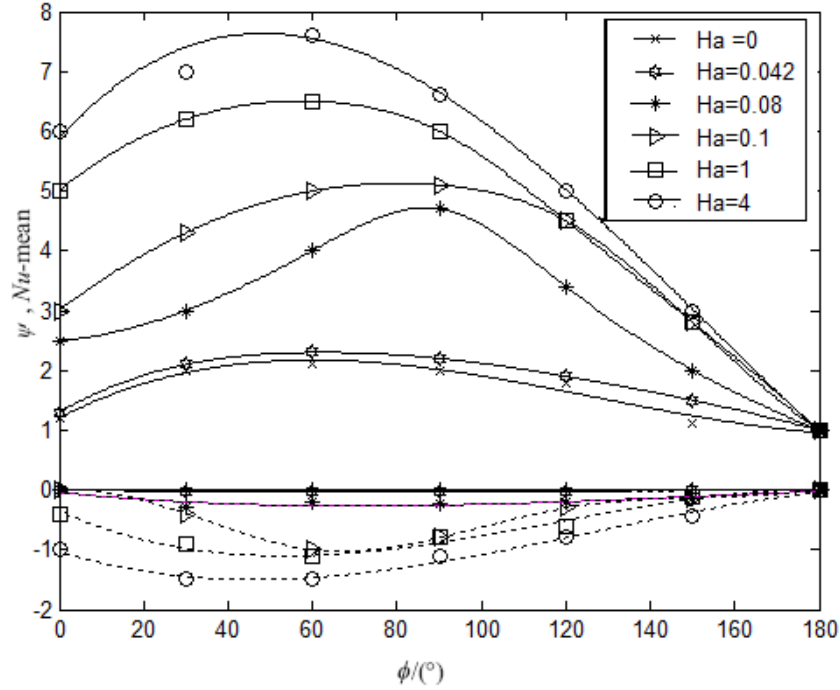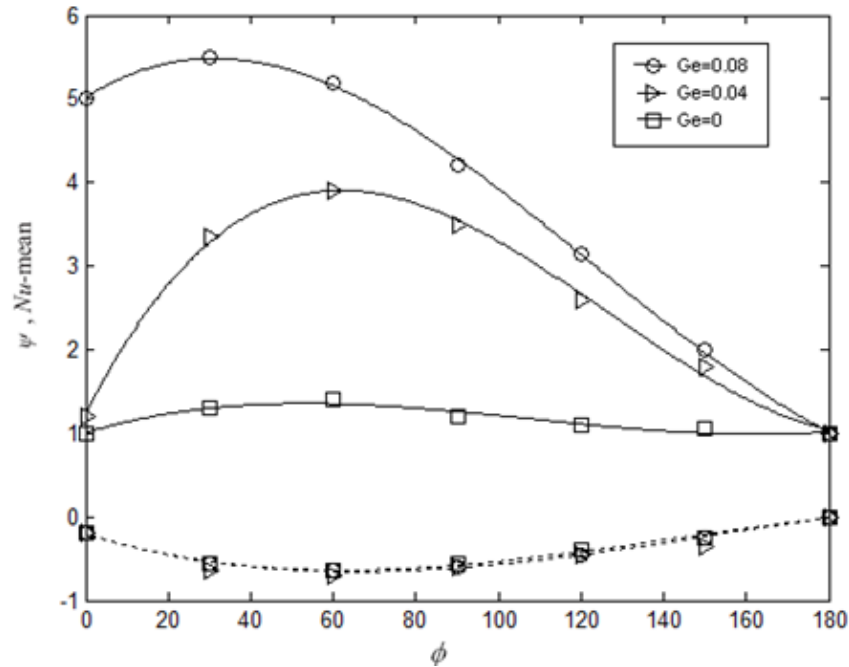Fig. 5.23 Variation of mean Nusselt number and dimensionless center-stream function with angle of inclination for an enclosure for various Ge for A = 1, For = 0.01, $Ra_w = 100$, and $Ha^2 = 0.02$

5.4 Forchheimer number effects:

Figures (5.24) illustrates the effect of Forchheimer number in the momentum equation on the dimensionless streamlines and isotherms patterns with other parameters unchanged, as it is shown, Forchheimer number has a certain effect on the heat flux and fluid flow by increasing the Forchheimer number the circulation of flow becomes in the upper portion of the enclosure and the dimension less stream function values are decreased; this is due to the increasing in the porosity inside the enclosure. On the other hand, the heat flux inside the enclosure becomes by conduction; due to decreasing in Nusselt number. Figure (5.25) shows the relation between the variations of mean Nusselt number with Forchheimer number. It can be seen that the mean

Nusselt number is decreased by increasing the Forchheimer number; this is due to decreasing in dimensionless temperature in the upper half region along the left-hand side and the lower half region along the right-hand side wall.
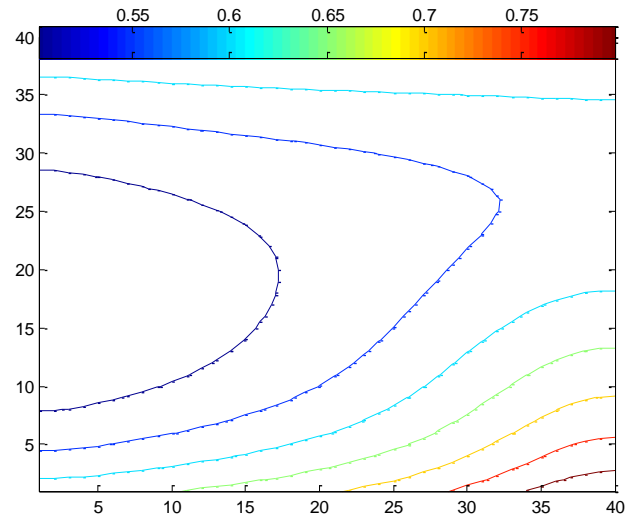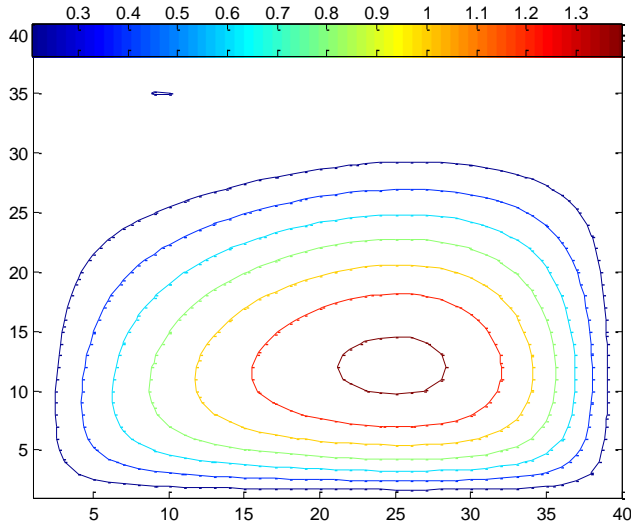
(a)
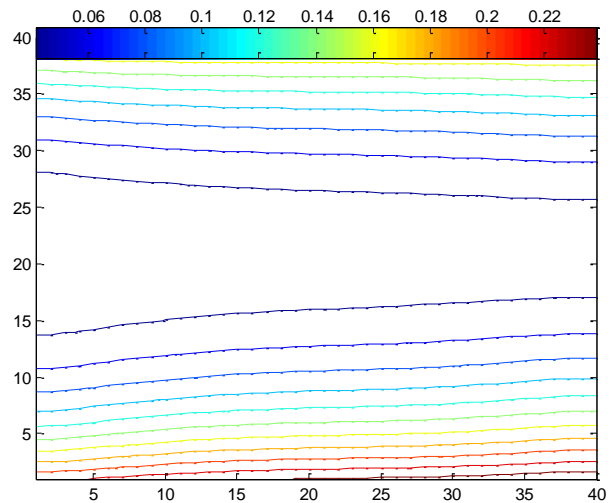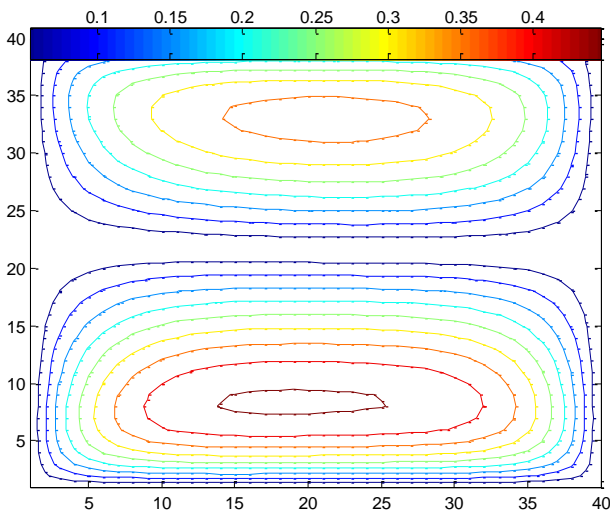
(b)
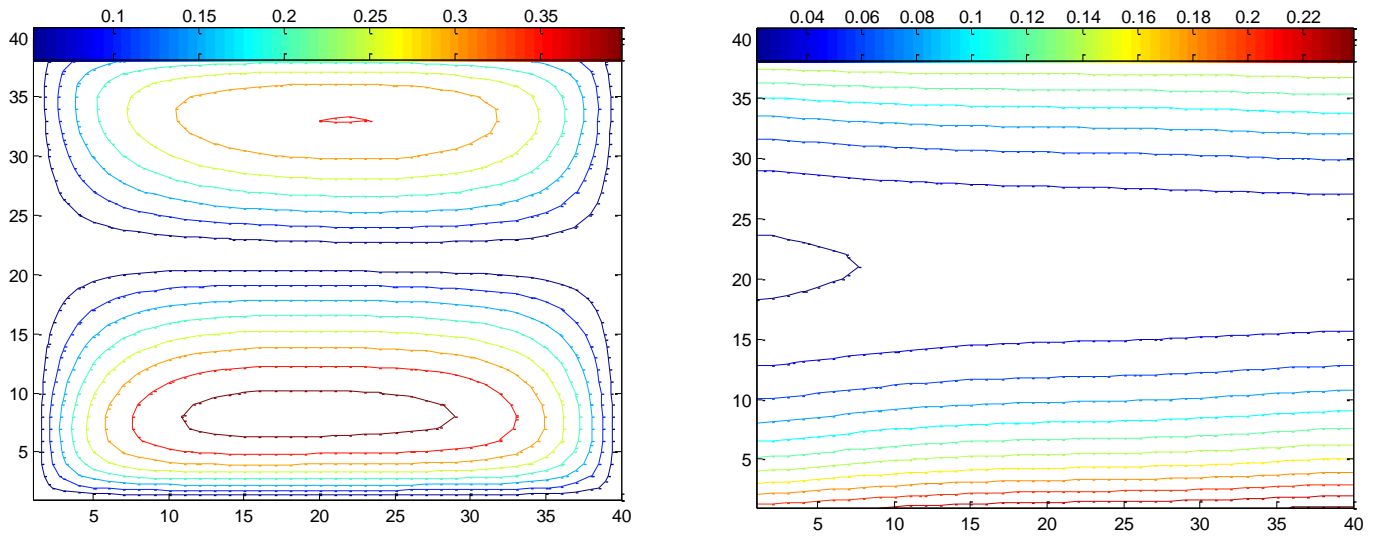
(c)

Fig. 5.24 Typical dimensionless streamline and dimensionless temperature patterns for various Forchheimer number (a) For=0, (b) For=0.008, (c) For=0.02, for $\phi = 30°$, A = 1, $Ha^2 = 0$, Ge=0, and $Ra_w = 100$
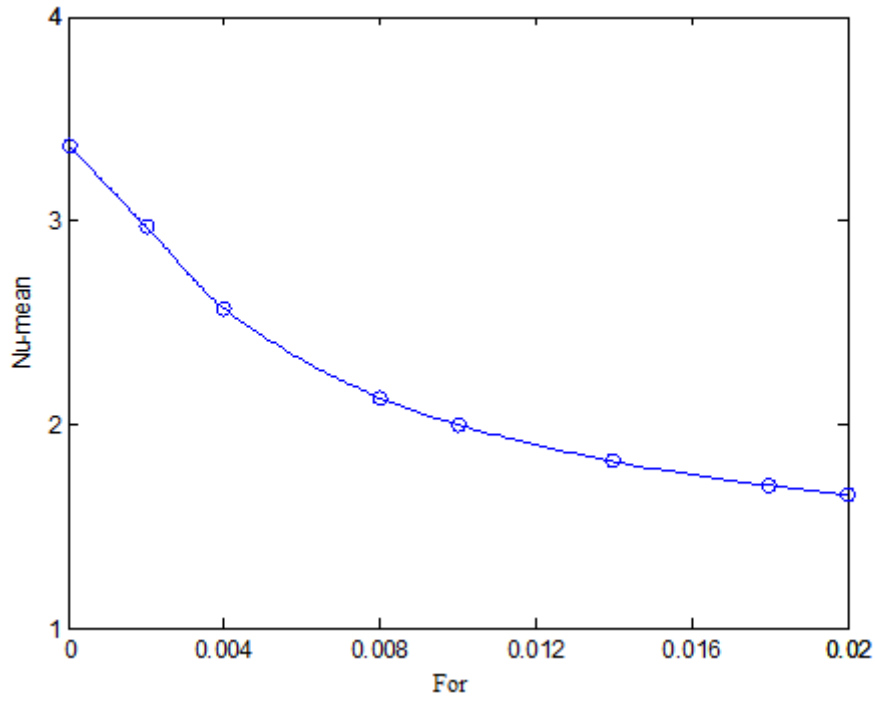
Fig. 5.25 Variation of Nu-mean with Forchheimer number for an enclosure for ϕ =30°, A = 1, $Ha^2 = 0$, Ge=0, and $Ra_w = 100$

Chapter 6

Conclusion and Recommendation

6.1 Conclusion:

In this study, the magnetohydrodynamics (MHD) natural convection heat transfer with Joule and viscous heating effects inside an iso-flux porous medium-filled inclined rectangular enclosure is studied numerically. An iso-heat flux is applied for heating and cooling the two opposing walls of the enclosure while the other walls are adiabatic. A finite difference scheme method was used. The conclusions can be obtained from previous results as a follow:

(1) The increasing magnetic influence number decreases the heat transfer coefficient and the fluid flow velocities, which is due to unfavorable retarding forces between the fluid layers.
 (2) The increasing the Gebhart number decreases heat transfer rates, which is due to the excessive heating of the fluid layers.

(3) The viscous and Joule heating effects depend directly on the Gebhart number.
.
(4) The heat flux rates and fluid flow velocities increase with the increase of the modified Rayleigh number.

(5) The Maximum heat transfer rates are obtained for inclination angels nearly 60°.

(6) As the aspect ratio increases, both the heat flux and fluid velocities decrease, which is due to the unfavorable thermal resistance inside the enclosure.

6.2 Recommendations:

In this study, the MHD-natural convection iso-flux interaction inside rectangular porous filled enclosures are going to be formulated using continuity, with Six-parameters are found to describe the problem under consideration namely; The non-Darcy effect parameter, the gravitational effect parameter, inclination angle parameter, magnetic effect parameter and the viscous heating effect parameter.

The following suggestions for further investigation based on the previous work are recommended:

1. Studying the problem with variations of both velocity and temperature fields in time.
2. Studying the effect of changing the boundary condition.
3. Studying the problem with add another term to the governing equations, such as the analogous to the Laplacian term that appears in the Navier-Stokes equation.

REFERENCES

Al-Zubi, Morad and H. M. Duwairi. (2007). **MHD Convection over non Isothermal Ellipse Embedded in Fluid Saturated Porous Medium**, Int. J. Heat and Technology, in press, vol. 25.

Aldoss, T. K., AI-Namir, M. A., Jarrah, M. A., and AI-Sha'er, B. J. (1995), **Magnetohydrodynamic mixed convection from a vertical plate embedded in a porous medium**, Numerical Heat Transfer, part A, vol. 28, pp. 635-645.

Badruddin, Z.A. Zainal, P.A. Aswatha Narayana, K.N. Seetharamu. (2006), **The steady state heat transfer in a porous medium fixed in a vertical annular cylinder**. International Journal of Heat and Mass Transfer, Volume 49, Issues 25-26, December 2006, Pages 4955-4965.

Batchelor, G.K. Introduction to Fluid Dynamics, Cambridge University Press.(1993).

Bilgen ,Z.G. Du, E. (1992), **Natural convection in vertical cavities with internal heat generating porous medium**, Warmeund Stoffubertr.,pp 149–155.

Boussinesq, J. (1903). **Th´eorie Analytique de la Chaleur, Gauthier-Villars, Paris**. vol. 2.

Chandra, B. and Gosh, N. (2001), **MHD flow of a visco-elastic liquid through porous - medium**, International Journal of Numerical Methods for Heat and Fluid, vol. 11, pp. 682-698.

Duwairi, H. M. and Damseh, R. A. (2004, a), **Magnetohydrodynamic natural convection heat transfer from radiate vertical porous surfaces**, Heat and Mass Transfer, vol. 40, pp. 787-792.

Duwairi, H. M. and Duwairi, R. M. (2004, b), **Thermal radiation effects on MHD-Rayleigh flow with constant surface heat flux**, Heat Mass Transfer, vol. 41, pp. 51-57.

Duwairi H. M. and Sufian Al-Araj (2004 c), **MHD-Mixed Convection Along Radiant Vertical Cylinder**, Conference of thermal Engineering: Theory and Application, 31/5-4/6, Lebanon.

Duwairi H. M., Rebhi. A. Damseh and Bourhan Tashtoush. (2006), **Transient Non-Boussinesq MHD-Free Convection Flows Over a Vertical Surface**. Int. J. Fluid Mechanics Research, vol. 2, pp.173-152.

Duwairi H. M. and Y. Al-Kablawi. (2006), **MHD-Conjugate Mixed Convection Heat Transfer Over a Vertical Hollow Cylinder Embedded in a Porous Medium**, Int. J. of Heat and Technology, vol. 24, pp. 123-128.

Ergun, S. (1952). **Fluid flow through packed columns**. Chem. Engrg. Prog. 48, 89–94.

Forchheimer, P. (1901), **Wasserbewegung durch Boden**, Zeitschrift des Vereines Deutscher Ingenieure 45, 1736–1741 and 1781–1788.

Garandet, J. P., Alboussiere, T. and Moreau, R. (1992), **Buoyancy driven convection in a rectangular enclosure with a transverse magnetic field**, Int.J. Heat Mass Transfer, vol. 35, pp. 741-749.

Hammad, I. M. and H. M. Duwairi (2008), **Mixed Convection Heat Transfer for a non-Newtonian Fluid around a Cylinder or Sphere Embedded in Porous Media**, Int. J. Heat and Technology, in press.

Henoch, C. W. and Meng, J. C. S. (1991), **Magnetohydrodynamic turbulent boundary layer control using external direct current crossed surface poles**, ASME, vol. 5(3), pp.115-121.

Hossain, M. A. (l992), **Viscous and Joule heating effects on MHD-free convection flow with variable plate temperature**, Int. J. Heat Mass Transfer, vol. 35, pp. 3485-3487.

Holman, J. A. (1990). **Heat Transfer, Ch12**. Newyork: McGraw-Hill Co.

Jha, B. K. (2001), **Natural convection in unsteady MHD Couette flow**, Heat and Mass Transfer, vol. 37, pp. 329-331.

Joseph, D. D. (1976). **Stability of Fluid Motions II**, Springer, Berlin.

Joseph, D. D., Nield, D. A. and Papanicolaou, G. (1982), **Nonlinear equation governing flow in a saturated porous medium**, Water Resources Res. 18, pp. 1049–

1052 and 19, 59.

Kim, S. and Lee, C. (2000), **Numerical investigation of cross flow around a circular cylinder at a low-Reynolds number flow under an electromagnetic force**, Experiments in Fluids, vol. 28, pp. 252-260.

Lage, J. L. (1998), **The fundamental theory of flow through permeable media: from Darcy, (to turbulence. Transport Phenomena in Porous Media** (eds. D.B. Ingham and I. Pop Elsevier, Oxford, pp.1–30.

Nield, P. A. and Bejan, A. (1999), **Convection in Porous Media, (2nd ed.)**, New York:Springer-verlag.

Oberbeck,A.(1879). **Ueber die W¨armeleitung der Fl¨ussigkeiten bei Ber¨ucksichtigung der Str¨omungen infolge von Temperaturdifferenzen**. *Ann. Phys. Chem.* **7**, 271–292.

Oosthuizen, P.H. and D.Naylor (1973), **An Introduction to convective heat transfer analysis**, McGraw-Hill, New York, NY.

Raptis, A. and Singh, A. K. (1983), **MHD free convection flow past an accelerated vertical plate**, Int. Comm. Heat Mass Transfer, vol. 10, pp.313-321.

Shehadeh F. G and Duwairi H. M, **MHD natural convection in porous media-filled enclosures** Appl. *Math. Mech. -Engl. Ed.* 30(9), 1113-1120 (2009).

Sparrow, E. M. and Cess, R. D. (1961), **Effect of magnetic field on free convection heat transfer**, Int. J. Heat Mass Transfer, vol. 3, pp.267-273.

Vasseur,P.Satish,M.G and Robillard,L, **Natural convection in a thin, inclined, porous layer exposed to constant heat flux** . *Int. J. Heat Mass Tran.*,Vol 30 No3,pp.537-549 (1987).

APPENDIX

- **Computer programme (MATLAB 7.0)**

```matlab
clear all;
clc;
% giving inputs
dx = 0.01; % [m]
dy = 0.01; %[m]
w =0.4 ; % [m]
h = 0.4; % [m]
fai=pi/3;
Ha =4;
CF = 0.01;
raw=100;
GE =0.05;
r = 0.9;
% calculating dX dY A
dX = dx/w;
dY = dy/h;
A =1;
M = (w/dx);
N = (h/dy);
Q = 0.5;     %Q2/Q1
% Applaying bounday condition for theta [ q1 heat flux & q2 heat flux walls ]
for i = 1:1:M
    for j = 1:1:N
        th(i,j)= 0;

    end
end


% Appaying Boundary condition for stream function

for i =1:1:M
    St(i,1) = 0;
    St(i,N) = 0;
end
for j =1:1:N
    St(1,j) = 0;
    St(M,j) = 0;
end
% For calcaulate theta and stream function at the nodes inside the encluser
done=0;
    while~done
    for i=2:1:M-1;
        for j=2:1:N-1;
```

```
    sss=1;
     keep = th(i,j);
     E1 = (th(i+1,j)+th(i-1,j))/(dX^2);
     E2 = (th(i,j+1)+th(i,j-1))/(dY^2);
     E3 = GE*Ha*(((St(i,j+1)-St(i,j-1))/(dY*2))^2);
     E4 = (GE*((St(i,j+1)-St(i,j-1))/(dY*2)))*(((St(i,j+1)-St(i,j-1))/(dY*2))+
     (CF*(     (   (St(i,j+1)-St(i,j-1))/(dY*2)      )^2      )));
     E5 = ((St(i+1,j)-St(i-1,j))/(dX*2))      *     ((th(i,j+1)-th(i,j-1))/(dY*2));
     E6 = ((St(i,j+1)-St(i,j-1))/(dY*2))   * ((th(i+1,j)-th(i-1,j))/(dX*2));
     E7 = (2/(dX^2))+(2/(dY^2));
     thcalc = (E1+E2+E3+E4+E5-E6)/(E7);
     th(i,j) =  keep + (  (r)*(thcalc-keep)  );
     th(i,1) = ((4*th(i,2)-th(i,3))/3);
     th(i,N) = ((4*th(i,N-1)-th(i,N-2))/3);
th(1,j)  = ((4*th(2,j)-th(3,j)+ (2*dX))/3);
th(M,j)  = (((Q) *( 2*dX)+4*th(M-1) -th(M-2,j))/3) ;

     keepSt = St(i,j);
       B1 = (St(i,j+1)+St(i,j-1))/(dY^2);
       B2 = (St(i+1,j)+St(i-1,j))/(dX^2);
       B3 =  2 * CF * ((St(i,j+1)-St(i,j-1))/(dY*2))* ((St(i,j+1)+St(i,j-1))/(dY^2));
       B4 = Ha *   (    ((((St(i,j+1)+St(i,j-1))/(dY^2)))* cos(fai))+
       (((((St(i+1,j)-St(i-1,j))/(dX^2)))* sin(fai))   ) ;
       B5 = raw *    (    (((th(i,j+1)-th(i,j-1))/(dY*2))*(cos(fai)))-
       (((th(i+1,j)-th(i-1,j))/(dX*2))*(sin(fai)))    ) ;
       B6 = (2/dY^2) +  (2/dX^2)  + (    ((2*CF)/dY^2)*((St(i,j+1)-St(i,j-1))/(dY)) )
       +(((2*Ha)/(dX^2))*(sin(fai))   ) +   (    ((2*Ha)/(dY^2))*(cos(fai))   ) ;
       Stcalc = (B1+B2+B3+B4-B5)/(B6);
          St(i,j) =  keepSt + (  (r)*(Stcalc-keepSt)  );
             eSt(i,j) = abs(St(i,j) -  keepSt);
           done=(eSt(i,j) <=0.0000005);
       end
       end

       end
```

```matlab
th(1,1) = th(1,2);
        th(M,1) = th(M,2);
        th(1,N) = th(1,N-1);
        th(M,N) = th(M,N-1);
Stabs=abs(St);
thabs=abs(th);
 %Nuselt number at left wall
    for j=1:1:N
        Nu(1,j)=1/th(2,j);
         end
%Nuselt number at right wall
    for j=1:1:N
       Nu(M,j)=(1/th(M-1,j))*(Q)
         end
 %Mean Nuselt number at left wall
f1=(Nu(1,1)/2);
f2=0;
    for j=2:1:N-1
        keepf2=f2;
        f2=Nu(1,j);
      f2=f2+keepf2;
    end
  f3=(Nu(1,N)/2);
  Nu_meanH=(dY/A)*(f1+f2+f3);

  _
   %Mean Nuselt number at right wall
g1=(Nu(M,1)/2);
g2=0;
    for j=2:1:N-1
        keepg2=g2;
        g2=Nu(M,j);
      g2=g2+keepg2;
    end
 g3=(Nu(M,N)/2);
 Nu_meanC=(dY/A)*(g1+g2+g3);
```

الحمل الحراري الطبيعي الكهرومغناطيسي في جسم محصور ثابت الإشعاع مملوء بوسط مسامي

إعداد

يوسف محمد جبر علي البدوي

المشرف

الاستاذ.الدكتور حمزة الدويري

ملخص

في هذا العمل الحمل الحراري الطبيعي الكهرومغناطيسي في وسط مسامي يملأ جسم محصور مستطيل الشكل ومائل بزاوية بظهور تأثير كل من الحرارة الناتجة من الجول واللزوجة سيتم البحث عنها numerically. حدود الجسم المحصور وضعت بحيث يكون جدارين adiabatic و الآخرين isothermal. معادلات العزم والطاقة سيتم تحويلها إلى dimensionless form باستخدام متغيرات معينة وبعد ذلك سيتم حلها باستخدام finite difference scheme. The governing parameters هي تأثير الحمل المغناطيسي و تأثير رقم جيبهارت و تأثير Rayleigh number وتأثير الزاوية وتأثير نسبة الطول للعرض للجسم المحصور. النتائج التي تم الحصول عليها بينت نقصان إنتقال الحرارة و جريان المائع بزيادة الحمل المغناطيسي ولقد تبين أنه بزيادة Rayleigh number ونسبة الطول للعرض للجسم المحصور سوف يزداد كل من إنتقال الحرارة و جريان المائع. بزيادة Gebhart number سوف يزداد كل من إنتقال الحرارة و جريان المائع.